



ELSEVIER

Journal of Chromatography A, 855 (1999) 455–486

JOURNAL OF
CHROMATOGRAPHY A

www.elsevier.com/locate/chroma

Molecular mechanism of retention in reversed-phase high-performance liquid chromatography and classification of modern stationary phases by using quantitative structure–retention relationships

Roman Kaliszan^a, Marion A. van Straten^b, Michal Markuszewski^a, Carel A. Cramers^b,
Henk A. Claessens^{b,*}

^a*Department of Biopharmaceutics and Pharmacodynamics, Medical University of Gdańsk, Gen. J. Hallera 107, 80-416 Gdańsk, Poland*

^b*Laboratory of Instrumental Analysis, Department of Chemical Engineering and Chemistry, Eindhoven University of Technology, P.O. Box 513, 5600 MB Eindhoven, The Netherlands*

Received 1 February 1999; received in revised form 25 May 1999; accepted 14 June 1999

Abstract

Quantitative structure–retention relationships (QSRRs) were derived for logarithms of retention factors normalised to a hypothetical zero percent organic modifier eluent, $\log k_w$, determined on 18 reversed-phase high-performance liquid chromatography (RP-HPLC) columns for 25 carefully designed, structurally diverse test analytes. The study was aimed at elucidating molecular mechanism of retention and at finding an objective manner of quantitative comparison of retention properties and classification of modern stationary phases for RP-HPLC. Three QSRR approaches were employed: (i) relating $\log k_w$ to logarithms of octanol–water partition coefficient ($\log P$); (ii) describing $\log k_w$ in terms of linear solvation-energy relationship-based parameters of Abraham; (iii) regressing $\log k_w$ against simple structural descriptors acquired by calculation chemistry. All the approaches produced statistically significant and physically interpretable QSRRs. By means of QSRRs the stationary phase materials were classified according to the prevailing intermolecular interactions in the separation process. Hydrophobic properties of the columns tested were parametrized. Abilities of individual phases to provide contributions to the overall retention due to non-polar London-type intermolecular interactions were quantified. Measures of hydrogen-bond donor activity and dipolarity of stationary phases are proposed along with two other phase polarity parameters. The parameters proposed quantitatively characterize the RP-HPLC stationary phases and provide a rational explanation for the differences in retention patterns of individual columns observed when applying the conventional empirical testing methods. © 1999 Elsevier Science B.V. All rights reserved.

Keywords: Stationary phases, LC; Quantitative structure–retention relationships; Retention mechanisms

1. Introduction

Quantitative structure–retention relationships (QSRRs) are statistically derived relationships be-

*Corresponding author. Tel.: +31-40-2473-012; fax: +31-40-2453-762.

E-mail address: H.A.Claessens@tue.nl (H.A. Claessens)

tween the chromatographic parameters determined for a representative series of analytes in given separation systems and the quantities (i.e. descriptors) accounting for the structural differences among the analytes tested [1]. QSRRs are based on the commonly acknowledged linear free-energy relationships (LFERs). In the last two decades QSRRs have often been applied to [2]: (i) predict retention for a new solute; (ii) identify the most informative structural descriptors (regarding properties); (iii) gain insight into the molecular mechanism of separation operating in a given chromatographic system; (iv) evaluate complex physicochemical properties of analytes, other than chromatographic, e.g., their hydrophobicity; and (v) predict relative biological activities within a set of drugs and other xenobiotics as well as the material properties of individual members of a family of chemicals.

In recent years numerous reports have appeared on the application of QSRRs in comparative studies of retention properties of stationary phase materials for reversed-phase high-performance liquid chromatography (RP-HPLC). In such studies three main types of QSRR have been employed. The oldest one consists of regressing logarithms of retention factors ($\log k$) against the logarithms of *n*-octanol–water partition coefficients ($\log P$). Various RP-HPLC stationary phases have thus been compared aiming usually at the identification of a chromatographic system reproducing the slow-equilibrium octanol–water partition system. See for example Refs. [3–5].

The second type of QSRR is based on the solvatochromic comparison method and the so-called linear solvation energy relationships (LSERs). The approach was introduced to chromatography and extensively developed by Abraham et al. and Carr [6,7]. Some representative applications of this latter LSER-based approach to the RP-HPLC column characterization may be found in Refs. [8–14].

The third type of QSRR equation describes the $\log k$ values in terms of quantum chemical indices and/or other structural descriptors from calculation chemistry. Examples of an application of such an obtained QSRR for comparison of the RP-HPLC columns may be found in Refs. [1,10,15–17].

In view of the reports published it is evident that QSRRs can, in quantitative statistical terms, differentiate RP-HPLC stationary phases of different chemi-

cal nature of the organic ligand and/or organic and inorganic support. QSRRs can also demonstrate which kind of the analyte–stationary phase interactions are decisive for retention on individual columns. However, when stationary phase materials are compared that belong to the same chemical class, like hydrocarbon-bound silicas, the results obtained are ambiguous. The conclusion drawn by Tan et al. [9] and by Abraham et al. [11] is that the relative importance of analyte structural descriptors in QSRRs explaining isocratic retention does not differ much for the various hydrocarbonaceous silica stationary phases studied.

We decided to test the hypothesis that QSRRs can serve to differentiate objectively, in a quantitative manner, the silica-based stationary phases for RP-HPLC. To that aim we carefully designed the experiment taking the following into consideration.

First, instead of isocratic retention parameters, we decided to consider data normalized by extrapolation of the linear relationships between $\log k$ and the percentage of organic modifier in the eluent. Second, we used a predesigned series of structurally diversified test analytes. The solutes were selected such that the intercorrelations within the series were minimized among the individual analyte structural descriptors [5,18,19]. At the same time, the selection of test analytes provided a wide range and even distribution of individual structural descriptor values. Besides that, the series of analytes was large enough to assure statistical significance of the QSRR equations but still experimentally manageable. Third, the three types of above-mentioned QSRR were derived and compared for individual stationary phases under study. For the sake of comparison two non-silica-based stationary phases were included in the test series of phases: an alumina-based one and a rigid polymer one.

2. Experimental

2.1. Columns

The columns used in these tests were kindly provided by the manufacturers (Table 1) and are summarized in Tables 2 and 3 for the C_{18} and C_8 phases, respectively, together with some of their

Table 1
List of column manufacturers, column dimensions and abbreviations

Column	Manufacturer	Dimensions L × i.d. (mm × mm)	Abbreviation	No.
<i>C₁₈ columns</i>				
Zorbax RX-C18	Hewlett-Packard, Newport, DE, USA	150 × 4.6	RX	1
Polygasil-60-5-C18	Macherey-Nagel, Düren, Germany	125 × 4.6	Poly	2
Hypersil HyPURITY C18	Shandon HPLC, Runcorn, UK	150 × 4.6	HyPUR	3
Hypersil ODS	Shandon HPLC, Runcorn, UK	125 × 4.6	Hyper	4
Symmetry C18	Waters, Milford, MA, USA	150 × 4.6	Sym18	5
Purospher RP-18 e	Merck, Darmstadt, Germany	125 × 4	Puro	6
Kromasil KR100-5C18	Eka Nobel, Bohus, Sweden	150 × 4.6	Krom	7
Alltima C18 5U	Alltech, Deerfield, IL, USA	150 × 4.6	All	8
TSKgel OD-2PW	TosoHaas, Stuttgart, Germany	150 × 4.6	TPW	9
TSKgel ODS-80TS	TosoHaas, Stuttgart, Germany	150 × 4.6	TTS	10
Eclipse XDB-C18	Hewlett-Packard, Newport, DE, USA	150 × 4.6	XC18	11
Nucleosil 100-5 C18 HD	Macherey-Nagel, Düren, Germany	150 × 4	NuC18	12
<i>C₈ columns</i>				
Eclipse XDB-C8	Hewlett-Packard, Newport, DE, USA	150 × 4.6	XC8	13
SymmetryShield RP8	Waters, Milford, MA, USA	150 × 4.6	Sym8	14
LiChrospher RP-Select B	Merck, Darmstadt, Germany	125 × 4	SelB	15
Aluspher RP-Select B	Merck, Darmstadt, Germany	125 × 4	Alu	16
Nucleosil 100-5 C8	Macherey-Nagel, Düren, Germany	150 × 4	NuC8	17
Nova-Pak C8	Waters, Milford, MA, USA	150 × 3.9	Nova	18

physicochemical properties. For practical reasons the methacrylate copolymer column (TPW) is placed in the list of C₁₈ columns and the polybutadiene coated column (Alu) is placed in the list of C₈ columns.

2.2. Equipment

Chromatographic measurements were made using a HP 1100 liquid chromatograph (Hewlett-Packard, Waldbronn, Germany), consisting of a quaternary pump, autosampler, column oven and diode array detector. HP ChemStation software was used for process control and data handling.

The injected sample volume was 1 µl. In all chromatographic investigations the flow rate was 1.0 ml/min except for the TPW column, where the flow rate was 0.5 ml/min. Columns were thermostatted at a temperature of 40°C.

2.3. Chemicals

Methanol and acetonitrile (supra-gradient grade)

were from Biosolve (Bio-Lab, Jerusalem, Israel). Water was prepared with a Milli-Q water purification system (Millipore, Milford, MA, USA).

Phosphate buffer with a concentration of 20 mM and pH of 3.0 was prepared with phosphoric acid and 1 M sodium hydroxide (Merck, Darmstadt, Germany). The analytes were 1,3,5-triisopropylbenzene, 1,4-dinitrobenzene, 3-trifluoromethylphenol, 3,5-dichlorophenol, 4-cyanophenol, 4-iodophenol, benzene, dibenzothiophene, indazole, 4-nitrobenzoic acid and toluene from Aldrich (Milwaukee, WI, USA); *n*-hexylbenzene, chlorobenzene, cyclohexanone, phenol, *N*-methyl-2-pyrrolidinone, 4-chlorophenol, 1,3-diisopropylbenzene were from Fluka (Buchs, Switzerland); methylphenylether, benzamide, hexachlorobutadiene, caffeine, naphthalene and benzoic acid were from Merck (Darmstadt, Germany) and benzonitrile was from Janssen (Beerse, Belgium). To obtain (1 µl injections) detector signals from 10 to 100 mAUFS, the concentrations of the test solutes were between 10 and 600 mg/l, except for cyclohexanone which was diluted 1:1 with methanol.

Table 2
List of tested C₁₈ columns and their physicochemical properties

	Column											
	RX	XC18	Puro	Hyper	HyPUR	Sym18	Poly	NuC18	Krom	All	TPW	TTS
Particle size (μm)	5.2	5	5.8	4.5–5	4.5	4.95	5.2	5.4	6.2	6.18	5	5
Pore size (C)	80	80	120	120	180	93	x	115	x	111.9	125	80
Pore volume (ml/g)	0.45	0.4	1.0	0.6	1.0	0.66	0.85	1.15	0.91	0.88	x	x
Surface area (m ² /g)	180	180	350	170	200	332	350	340	349	316	x	198
Carbon loading (%)	12	10.3	18	9.5	13	19.4	x	21.0	21.4	16.22	x	15
Surface coverage (μmol/m ²)	3.3	3.5	3.2	x	x	3.21	x	3.60	3.45	x	x	x
Bulk density (g/ml)	1.0	1.0	0.4	x	x	x	x	0.36	x	x	ca. 1	x
Bonded chemistry	Dimethyl-C ₁₈	Dimethyl-C ₁₈	Trifunctional	Trifunctional	Monofunctional	x	Not pure monomeric	Monomeric	Monofunctional	Polymeric	Monomeric	Monomeric
End capping	No	Double	Yes	Yes	Yes	x	x	Yes	Yes	Double	No	Yes
Silica	RX-sil	RX-sil							Polyester silica		Methacrylate copolymer	High purity

x: Data not available.

Table 3
List of tested C₈ columns and their physicochemical properties

	Column					
	XC8	SelB	Alu	Sym8	Nova	NuC8
Particle size (μm)	5	5.5	5	5.07	4	5.4
Pore size (C)	80	90	100	89	75	115
Pore volume (ml/g)	0.4	0.9	0.5	0.65	0.30	1.15
Surface area (m ² /g)	180	360	170	343	120	340
Carbon loading (%)	7.2	11.5	7	14.4	4.0	8.0
Surface coverage (μmol/m ²)	3.7	3.5	Coated	3.35	x	2.60
Bulk density (g/ml)	1.0	0.4	0.45	x	x	0.36
Bonded chemistry	Dimethyl-C ₈	Bifunctional	Polybutadiene	x	x	Monomeric
End capping	Double	No	No	x	Yes	No
Silica	RX-sil					

x: Data not available.

2.4. Procedures

Depending on their retention properties the analytes were chromatographed at five to eight compositions of mixtures of organic–water (or aqueous buffer) mobile phases ranging from 95:5 to 20:80 (v/v). Based on the linear relationships between the logarithm of retention factor ($\log k$) and the organic modifier concentration in the eluent, the values corresponding to 100% water or buffered eluent were obtained by extrapolation ($\log k_w$). The data are summarized in Table 4. For benzoic acid and 4-nitrobenzoic acid retention data are missing due to a lack of retention in non-buffered systems.

2.5. Selection of test analytes

A series of 25 test analytes were taken as previously designed [5] with the well-defined hydrogen-bond capacity descriptors derived from the complexation scales of Abraham [18,19].

2.6. Structural descriptors of analytes

The logarithms of *n*-octanol–water partition coefficients ($\log P$) can be found in the literature [20,21].

The LSER parameters of Abraham for the test analytes originated from Refs. [18,19]; these were used to derive the solvation equation of a general form:

$$\log AP = c + rR_2 + s\pi_2^H + a\alpha_2^H + b\beta_2^H + vV_x \quad (1)$$

where AP is a property for a series of analytes in a fixed solvent system (here k_w), R_2 is an excess molar refraction, π_2^H is the analyte dipolarity/polarizability, α_2^H and β_2^H are the analyte overall or effective hydrogen-bond acidity and basicity, respectively, and V_x is the McGowan characteristic volume. The coefficients c , r , s , a , b and v in Eq. (1) are characteristic of the systems (being the HPLC systems 1–42, from Table 4). They represent the difference in individual properties (complementary to R_2 , π_2^H , α_2^H , β_2^H and V_x) between the mobile and the stationary phase. Hence, r should be proportional to the difference between excess molar refractivity of the stationary and the mobile phase, s should reflect the corresponding differences in dipolarity/polarizability and v between the McGowan volumes. The coefficient a is assumed to be proportional to a difference in hydrogen-bond basicity between the stationary and the mobile phase and b is related to analogous difference in hydrogen-bond acidity.

The test analytes were subjected to molecular modeling by the HyperChem package with the extension ChemPlus (Hyper-Cube, Waterloo, Canada). In effect, a number of quantum chemical and standard additive/constitutive structural descriptors were generated. The following were significant in QSRRs: solvent (water)-accessible molecular surface area (SAS), square of total dipole moment (μ^2) and highest electron excess on a single atom in analyte molecule (δ_{\min}).

Table 4

Logarithms of retention factors extrapolated to pure water or buffered eluent as obtained in individual chromatographic systems studied; for experimental details see text

No.	Solute	$\log k_w$ C ₁₈ columns							
		RX				Hyper			
		1 MeOH–water	2 ACN–water	3 MeOH–buffer	4 ACN–buffer	5 MeOH–water	6 ACN–water	7 MeOH–buffer	8 ACN–buffer
1	<i>n</i> -Hexylbenzene	5.2338	3.6082	5.4892	3.4530	5.0981	3.3166	5.1382	3.3206
2	1,3,5-Triisopropylbenzene	6.0813	4.0707	6.0714	3.9240	5.9344	3.8010	5.9792	3.7951
3	1,4-Dinitrobenzene	1.5780	1.6050	1.5692	1.5886	1.4976	1.5188	1.5090	1.5491
4	3-Trifluoromethylphenol	2.4764	1.9136	2.5650	1.8849	2.5446	1.8089	2.5499	1.8180
5	3,5-Dichlorophenol	2.9071	1.8552	2.9099	1.7515	2.9028	2.0989	2.9048	2.0052
6	4-Cyanophenol	1.1916	0.9906	1.1786	0.7926	1.1868	0.7877	1.1986	0.7249
7	4-Iodophenol	2.3279	1.4667	2.3819	1.6917	2.3730	1.6518	2.3725	1.6531
8	Methylphenylether	2.0084	1.7162	2.0436	1.6386	1.9424	1.5997	1.9467	1.6012
9	Benzamide	0.7458	0.4002	0.8308	0.1295	0.7599	0.1081	0.7663	0.0984
10	Benzene	1.9661	1.7094	2.0052	1.7419	1.8808	1.6087	1.8934	1.5948
11	Chlorobenzene	2.6415	1.9819	2.6725	2.2091	2.5579	2.0530	2.5558	2.0272
12	Cyclohexanone	0.9586	0.8198	1.0396	0.6423	0.8369	0.5555	0.9568	0.6563
13	Dibenzothiophene	3.9230	2.6457	4.0185	2.8022	3.6125	2.8212	3.6744	2.7543
14	Phenol	1.0730	0.9182	1.0938	0.8133	1.1348	0.7890	1.1375	0.7659
15	Hexachlorobutadiene	4.4606	3.1651	4.5311	3.0702	4.3737	2.8572	4.3841	2.9508
16	Indazole	1.6297	1.0743	1.6175	0.6505	1.5651	0.7710	1.5684	0.7844
17	Caffeine	0.8002	−0.3913	0.8923	−0.3868	0.5884	−0.5872	0.5844	−0.3064
18	4-Nitrobenzoic acid		−0.3980	1.5758	0.9011			1.7651	1.1752
19	<i>N</i> -Methyl-2-pyrrolidinone	0.3626	−0.4250	0.3015	−0.2504	−0.0126	−0.5196	−0.0304	−0.4958
20	Naphthalene	3.0420	2.2951	3.0787	2.3060	3.0422	2.2422	3.0259	1.8410
21	4-Chlorophenol	1.9309	1.4386	1.9694	1.4452	1.9458	1.3629	1.9495	1.3710
22	Toluene	2.5774	2.0040	2.6125	1.9952	2.4506	2.0257	2.4584	2.0333
23	Benzonitrile	1.5309	1.4170	1.5680	1.2976	1.5357	1.2402	1.5969	1.2298
24	Benzoic acid		0.1298	1.6027	0.8296			1.6578	0.7732
25	1,3-Diisopropylbenzene	4.8603	3.3848	4.8854	3.2503	4.7017	3.3468	4.7314	3.1553

Table 4. (Continued)

No.	Solute	log k_w C ₁₈ columns							
		Poly				All			
		9 MeOH–water	10 ACN–water	11 MeOH–buffer	12 ACN–buffer	13 MeOH–water	14 ACN–water	15 MeOH–buffer	16 ACN–buffer
1	<i>n</i> -Hexylbenzene	5.1998	3.3679	5.1861	3.3400	5.4057	3.7257	5.3850	3.6931
2	1,3,5-Triisopropylbenzene	6.0459	3.8323	6.0368	3.7883	6.2520	4.2157	6.2455	4.1760
3	1,4-Dinitrobenzene	1.6620	1.5914	1.6202	1.5355	1.8268	1.8647	1.8004	1.8521
4	3-Trifluoromethylphenol	2.6449	1.8378	2.5922	1.7563	2.8198	2.1023	2.7923	2.0871
5	3,5-Dichlorophenol	3.0549	2.0672	2.9463	1.9916	3.1162	2.3416	3.0997	2.3250
6	4-Cyanophenol	1.3316	0.8123	1.2880	0.7335	1.4863	1.0926	1.4632	1.0694
7	4-Iodophenol	2.4727	1.7038	2.4236	1.6250	2.6019	1.9523	2.5771	1.9369
8	Methylphenylether	2.1481	1.6778	2.0992	1.6168	2.2261	1.9168	2.2068	1.9090
9	Benzamide	0.8519	0.1278	0.7770	0.0861	0.9358	0.3617	0.9922	0.3606
10	Benzene	2.0716	1.6850	2.0222	1.6274	2.2190	1.9143	2.1990	1.9062
11	Chlorobenzene	2.7822	2.1447	2.5718	2.0708	2.8350	2.3381	2.8016	2.3282
12	Cyclohexanone	1.0827	0.6528	1.0266	0.6166	1.1670	0.9032	1.2075	0.9024
13	Dibenzothiophene	3.8388	2.9375	3.7882	2.8702	4.0164	2.9297	3.9759	2.9152
14	Phenol	1.1966	0.8112	1.1970	0.8325	1.3910	1.0752	1.3808	1.0710
15	Hexachlorobutadiene	4.4550	3.0965	4.4056	2.9910	4.5940	3.2736	4.5590	3.2508
16	Indazole	1.6737	0.8301	1.6080	0.7748	1.7168	1.0582	1.7010	1.0502
17	Caffeine	0.7839	−0.2164	0.8473	−0.1710	0.7959	−0.0591	0.7853	−0.0548
18	4-Nitrobenzoic acid			1.9033	0.8934		0.2632	1.9827	1.1980
19	<i>N</i> -Methyl-2-pyrrolidinone	0.1961	−0.4412	0.1951	−0.4445	−0.1499	−0.3067	0.1586	−0.3081
20	Naphthalene	3.2751	2.2702	3.0322	2.1879	3.2693	2.5274	3.2419	2.5068
21	4-Chlorophenol	2.0377	1.3949	1.9843	1.3369	2.2100	1.6592	2.2017	1.6450
22	Toluene	2.7155	2.1047	2.6132	2.0346	2.7706	2.3435	2.7446	2.3337
23	Benzonitrile	1.6937	1.3140	1.6792	1.2613	1.7757	1.5540	1.7625	1.5453
24	Benzoic acid			1.6673	0.7811	1.0300	0.6692	1.8317	1.0783
25	1,3-Diisopropylbenzene	4.7653	3.3025	4.7261	3.1841	4.9858	3.4694	4.9695	3.4371

(Continued on next page)

Table 4. (Continued)

No.	Solute	log k_w C ₁₈ columns							
		TPW				XC18			
		17 MeOH–water	18 ACN–water	19 MeOH–buffer	20 ACN–buffer	21 MeOH–water	22 ACN–water	23 MeOH–buffer	24 ACN–buffer
1	<i>n</i> -Hexylbenzene	4.5554	3.0531	4.5786	3.0757	5.3558	3.5302	5.3376	3.6016
2	1,3,5-Triisopropylbenzene	5.1134	3.1800	5.1524	3.4579	6.2302	4.0454	6.1974	4.1013
3	1,4-Dinitrobenzene	1.9694	1.7676	1.9512	1.7804	1.6859	1.6215	1.6510	1.5880
4	3-Trifluoromethylphenol	2.6812	1.9713	2.6149	1.9800	2.7126	1.8628	2.6800	1.8081
5	3,5-Dichlorophenol	3.0890	2.1992	3.0049	2.0060	3.0916	2.1041	3.0416	2.0521
6	4-Cyanophenol	1.6363	1.2072	1.6257	1.2094	1.3571	0.8200	1.3038	0.7984
7	4-Iodophenol	2.5661	1.8677	2.5058	1.9325	2.5310	1.7150	2.4992	1.6672
8	Methylphenylether	1.9025	1.6246	1.8863	1.6308	2.1241	1.6980	2.1012	1.6636
9	Benzamide	0.8018	0.4559	0.7725	0.4230	0.8944	0.1159	0.7845	0.1027
10	Benzene	1.9084	1.6137	1.9094	1.6163	2.0713	1.6960	2.0527	1.6799
11	Chlorobenzene	2.5458	1.9939	2.4592	1.9840	2.7275	2.0019	2.6909	2.1145
12	Cyclohexanone	0.6929	0.5997	0.6963	0.5859	1.1377	0.6497	1.0095	0.6319
13	Dibenzothiophene	3.5255	2.4318	3.5433	2.3019	3.8679	2.6949	3.8550	2.6944
14	Phenol	1.4717	1.1286	1.4334	1.1242	1.2530	0.8311	1.2358	0.8105
15	Hexachlorobutadiene	3.9122	2.8109	3.9275	2.7180	4.0582	3.2258	4.4908	3.1971
16	Indazole	1.6433	1.1355	1.6461	1.1355	1.7198	0.7960	1.6358	0.7596
17	Caffeine	0.1500	0.1597	0.2118	0.3910	0.9536	−0.3041	0.9234	−0.3322
18	4-Nitrobenzoic acid			1.7778	1.2479			1.6974	0.9041
19	<i>N</i> -Methyl-2-pyrrolidinone	−0.5060	−0.4417	−0.526	−0.485	0.1840	−0.4981	0.1553	−0.4963
20	Naphthalene	2.9237	2.2006	2.8315	2.1607	3.1416	2.3088	3.0769	2.3118
21	4-Chlorophenol	2.2752	1.6010	2.2430	1.5981	2.0994	1.4162	2.0715	1.3723
22	Toluene	2.3733	1.9073	2.3231	1.9203	2.6969	2.1493	2.6617	2.1053
23	Benzonitrile	1.5656	1.3178	1.5459	1.3145	1.6546	1.3078	1.6031	1.2792
24	Benzoic acid			1.6381	1.1422			1.7365	0.8084
25	1,3-Diisopropylbenzene	4.1358	2.8004	4.1570	2.9394	4.9206	3.2867	4.9064	3.3368

Table 4. (Continued)

No.	Solute	log k_w C ₁₈ columns					
		HyPUR	Krom	NuC18	Puro	Sym18	TTS
		25 MeOH–water	26 MeOH–water	27 MeOH–water	28 MeOH–water	29 MeOH–water	30 MeOH–water
1	<i>n</i> -Hexylbenzene	4.7107	5.2190	5.1271	5.3069	5.1909	5.1209
2	1,3,5-Triisopropylbenzene	5.4266	6.0212	5.9329	6.1190	6.0092	5.9649
3	1,4-Dinitrobenzene	1.3676	1.7052	1.6220	1.6678	1.6602	1.6566
4	3-Trifluoromethylphenol	2.4416	2.8016	2.6547	2.6896	2.7466	2.6647
5	3,5-Dichlorophenol	2.7585	3.0755	2.9964	3.0018	3.0946	2.9880
6	4-Cyanophenol	1.1301	1.4036	1.3167	1.2731	1.3496	1.3421
7	4-Iodophenol	2.3120	2.6041	2.4809	2.5052	2.5664	2.4875
8	Methylphenylether	1.7989	2.1574	2.0460	2.2153	2.1217	2.0657
9	Benzamide	0.6055	0.8829	0.8461	0.8063	0.8526	0.8506
10	Benzene	1.7305	2.1138	1.9917	2.1618	2.0816	1.9870
11	Chlorobenzene	2.3847	2.7667	2.5912	2.8284	2.7238	2.6353
12	Cyclohexanone	0.8279	1.1424	1.0625	1.1123	1.1131	1.0651
13	Dibenzothiophene	3.4235	3.8734	3.7405	3.9712	3.8180	3.7396
14	Phenol	1.0449	1.3342	1.1913	1.2442	1.2995	1.2479
15	Hexachlorobutadiene	3.9871	4.4771	4.4093	4.5269	4.4292	4.3749
16	Indazole	1.3355	1.6188	1.6408	1.5563	1.6591	1.5537
17	Caffeine	0.3371	0.7457	0.9215	0.6950	0.7106	0.8007
18	4-Nitrobenzoic acid					2.4472	
19	<i>N</i> -Methyl-2-pyrrolidinone	−0.1811	0.0897	0.1323	0.0597	0.0989	0.1029
20	Naphthalene	2.5951	3.0234	3.0204	3.2237	3.1064	3.0239
21	4-Chlorophenol	1.8907	2.1811	2.0622	2.0845	2.1442	2.0711
22	Toluene	2.3081	2.7042	2.5851	2.7517	2.6639	2.5723
23	Benzonitrile	1.3329	1.6503	1.5589	1.6996	1.6198	1.6179
24	Benzoic acid					1.9457	
25	1,3-Diisopropylbenzene	4.3683	4.8088	4.7141	4.8720	4.7750	4.6473

(Continued on next page)

Table 4. (Continued)

No.	Solute	log k_w C ₈ columns							
		SelB				Alu			
		31 MeOH–water	32 ACN–water	33 MeOH–buffer	34 ACN–buffer	35 MeOH–water	36 ACN–water	37 MeOH–buffer	38 ACN–buffer
1	<i>n</i> -Hexylbenzene	4.6373	3.3923	4.5355	3.3191	4.1126	2.8848	3.9777	2.6084
2	1,3,5-Triisopropylbenzene	5.3220	3.6354	5.1902	3.7910	4.2995	3.5542	4.5180	2.8828
3	1,4-Dinitrobenzene	1.3461	1.5331	1.3674	1.5522	0.6438	0.6132	0.6737	0.7126
4	3-Trifluoromethylphenol	2.3647	1.7886	2.3670	1.8305	1.6000	1.3916	1.5095	1.1560
5	3,5-Dichlorophenol	2.6839	1.9453	2.6841	1.9600	2.3616	1.7839	2.1974	1.6878
6	4-Cyanophenol	1.2583	0.9432	1.2891	0.9358	0.6948	0.6399	0.5895	0.1968
7	4-Iodophenol	2.1779	1.6259	2.1672	1.6449	1.7375	1.5761	1.5762	1.3899
8	Methylphenylether	1.7501	1.5375	1.7991	1.5648	1.0251	0.9442	1.0749	0.8667
9	Benzamide	0.7141	0.3215	0.7799	0.2902	−0.2062	−0.0985	−0.1402	−0.2770
10	Benzene	1.6443	1.5155	1.6509	1.5443	1.0147	0.9847	1.1995	0.8956
11	Chlorobenzene	2.2602	1.8989	2.2645	1.9254	1.6918	1.5385	1.8712	1.4445
12	Cyclohexanone	0.8361	0.6733	0.8754	0.6654	−0.3073	−0.2962	−0.3037	−0.2804
13	Dibenzothiophene	3.4309	2.5668	3.4118	2.5602	3.2115	2.3651	3.1116	2.2829
14	Phenol	1.0308	0.8845	1.0676	0.8900	0.3228	0.3173	0.2892	0.0228
15	Hexachlorobutadiene	4.0406	2.9490	4.0065	2.9503	3.5006	2.7396	3.4193	2.5917
16	Indazole	1.4825	0.9075	1.5021	0.9110	0.6433	0.6299	0.8012	0.5318
17	Caffeine	0.7163	−0.0256	0.7554	−0.0658	−0.4410	−0.2310	−0.3728	−0.2686
18	4-Nitrobenzoic acid			1.5201	0.8815			1.0909	0.7337
19	<i>N</i> -Methyl-2-pyrrolidinone	0.0880	−0.3006	0.1175	−0.2956	−1.1817	−1.0143		−1.0230
20	Naphthalene	2.7444	2.2082	2.7078	2.2437	2.2670	2.0121	2.3538	1.8208
21	4-Chlorophenol	1.8158	1.3834	1.8142	1.4126	1.2959	1.1225	1.1184	0.9322
22	Toluene	2.1584	1.8580	2.1586	1.9329	1.5060	1.4017	1.5525	1.2732
23	Benzonitrile	1.4824	1.2914	1.5091	1.3150	0.5406	0.4934	0.7521	0.4403
24	Benzoic acid			1.5297	0.9358			0.8847	0.4267
25	1,3-Diisopropylbenzene	4.2480	3.1634	4.1767	3.2848	3.5504	2.8448	3.4713	2.3494

Table 4. (Continued)

No.	Solute	log k_w C ₈ columns			
		Nova	NuC8	Sym8	XC8
		39 MeOH–water	40 MeOH–water	41 MeOH–water	42 MeOH–water
1	<i>n</i> -Hexylbenzene	4.7745	3.9645	4.4738	4.9374
2	1,3,5-Triisopropylbenzene	5.4878	4.7232	5.2525	5.9716
3	1,4-Dinitrobenzene	1.5069	1.1830	1.4522	1.5553
4	3-Trifluoromethylphenol	2.6256	2.0709	2.6178	2.7348
5	3,5-Dichlorophenol	2.9614	2.4038	3.0072	3.0692
6	4-Cyanophenol	1.3407	1.2072	1.4104	1.3311
7	4-Iodophenol	2.4061	1.9197	2.4404	2.5025
8	Methylphenylether	1.9239	1.5436	1.7442	2.0179
9	Benzamide	0.7741	0.6733	0.6872	0.8129
10	Benzene	1.8088	1.4001	1.7796	1.9522
11	Chlorobenzene	2.4383	1.9804	2.3556	2.5633
12	Cyclohexanone	1.0348	0.8221	0.7497	1.0410
13	Dibenzothiophene	3.5984	3.1741	3.4161	3.5152
14	Phenol	1.1858	0.8722	1.1608	1.2608
15	Hexachlorobutadiene	4.0621	3.5907	3.8267	4.2239
16	Indazole	1.6043	1.3478	1.4381	1.6585
17	Caffeine	0.6040	0.7581	0.4395	0.5841
18	4-Nitrobenzoic acid				
19	<i>N</i> -Methyl-2-pyrrolidinone	0.0162	0.1046	−0.3085	0.0172
20	Naphthalene	2.8672	2.4313	2.7105	2.8819
21	4-Chlorophenol	2.0041	1.5628	2.0363	2.0996
22	Toluene	2.3645	1.8661	2.1840	2.5072
23	Benzonitrile	1.5796	1.3772	1.4034	1.6055
24	Benzoic acid				
25	1,3-Diisopropylbenzene	4.4080	3.8485	4.1497	4.6166

Table 5
Structural descriptors of test analytes that were employed in QSRR equations^a

No.	Solute	Log <i>P</i>	<i>R</i> ₂	π_2^H	α_2^H	β_2^H	<i>V</i> _x	δ_{\min}	μ^2	SAS
1	<i>n</i> -Hexylbenzene	5.52	0.591	0.50	0.00	0.15	1.562	-0.2104	0.03880	415.40
2	1,3,5-Triisopropylbenzene		0.627	0.40	0.00	0.22	1.985	-0.2057	0.00624	478.27
3	1,4-Dinitrobenzene	1.47	1.13	1.63	0.00	0.41	1.065	-0.3418	0.00012	312.07
4	3-Trifluoromethylphenol	2.95	0.425	0.87	0.72	0.09	0.969	-0.2454	4.39321	302.54
5	3,5-Dichlorophenol	3.62	1.02	1.10	0.83	0.00	1.020	-0.2434	1.98246	306.77
6	4-Cyanophenol	1.60	0.94	1.63	0.79	0.29	0.930	-0.2440	10.9693	290.61
7	4-Iodophenol	2.91	1.38	1.22	0.68	0.20	1.033	-0.3021	2.51856	301.47
8	Methylphenylether	2.11	0.708	0.75	0.00	0.29	0.916	-0.2116	1.56000	288.13
9	Benzamide	0.64	0.99	1.50	0.49	0.67	0.973	-0.4334	12.8450	293.30
10	Benzene	2.13	0.61	0.52	0.00	0.14	0.716	-0.1301	0.00000	244.95
11	Chlorobenzene	2.89	0.718	0.65	0.00	0.07	0.839	-0.1295	1.70824	269.49
12	Cyclohexanone	0.81	0.403	0.86	0.00	0.56	0.861	-0.2944	8.83278	269.31
13	Dibenzothiophene	4.38	1.959	1.31	0.00	0.18	1.379	-0.2709	0.27457	364.54
14	Phenol	1.47	0.805	0.89	0.60	0.30	0.775	-0.2526	1.52028	256.72
15	Hexachlorobutadiene	4.78	1.019	0.85	0.00	0.00	1.321	-0.0750	0.06708	352.14
16	Indazole	1.77	1.18	1.25	0.54	0.34	0.905	-0.2034	2.39011	285.46
17	Caffeine	-0.07	1.5	1.60	0.00	1.35	1.363	-0.3620	13.3298	367.02
18	4-Nitrobenzoic acid	1.89	0.99	1.07	0.62	0.54	1.106	-0.3495	11.7786	321.77
19	<i>N</i> -Methyl-2-pyrrolidinone	-0.54	0.491	1.50	0.00	0.95	0.820	-0.3532	12.9168	270.53
20	Naphthalene	3.30	1.34	0.92	0.00	0.20	1.085	-0.1277	0.00000	313.25
21	4-Chlorophenol	2.39	0.915	1.08	0.67	0.20	0.898	-0.2482	2.18448	280.38
22	Toluene	2.73	0.601	0.52	0.00	0.14	0.716	-0.1792	0.06916	274.50
23	Benzonitrile	1.56	0.742	1.11	0.00	0.33	0.871	-0.1349	11.1222	277.91
24	Benzoic acid	1.87	0.73	0.90	0.59	0.40	0.932	-0.3651	5.85156	288.00
25	1,3-Diisopropylbenzene		0.605	0.46	0.00	0.20	1.562	-0.2055	0.08820	399.79

^a Log *P* = Logarithm of *n*-octanol–water partition coefficient; *R*₂ = excess molar refraction, π_2^H = dipolarity/polarizability, α_2^H = hydrogen-bond acidity, β_2^H = hydrogen-bond basicity, *V*_x = characteristic volume of McGowan, δ_{\min} = highest electron excess charge on an atom in the analyte molecules (in electrons), μ^2 = square of total dipole moment (in Debyes), SAS = solvent (water)-accessible molecular surface area (in Å²).

The structural descriptors considered in final QSRR equations are listed in Table 5.

2.7. Statistical analysis

Calculations employing the Statgraphics Plus-6.0 package (Manugistics, Rockville, MD, USA) were run on a personal computer. The procedures of stepwise regression, multiple regression and principal component analysis were executed keeping the requirements of the meaningful quantitative structure activity relationship (QSAR) statistics [22] in mind.

3. Results and discussion

We decided to consider the log *k*_w data instead of individual isocratic log *k* data in the QSRR studies. The log *k*_w parameter is a standardized retention

parameter that is more reliable than any arbitrarily selected isocratic log *k* [1]. With the isocratic log *k* data the problem would arise which compositions of methanol–water and acetonitrile–water mixtures should be chosen for a comparative QSRR study. The log *k*_w cannot be considered as a retention parameter that would ever emerge if elution with pure water or buffer was experimentally possible. The log *k*_w basically is an abstract quantity. It is the intercept of the linear Soczewinski relationship [23] between isocratic log *k* values and the corresponding volume percent of organic modifier in eluent. It is known that log *k*_w depends on the nature of organic modifier of the binary aqueous eluents employed in RP-HPLC [24].

As is evident from Table 4, the log *k*_w data extrapolated from methanol–water systems are larger than the respective data from the acetonitrile–water systems. This fact reflects the steeper decrease in log

k with increasing methanol concentration in methanol–water mobile phases than is the case with acetonitrile–water eluents. This may be explained in view of the observations [25–27] that organic modifiers solvate the hydrocarbonaceous stationary phases differently that are used in RP-HPLC. As acetonitrile adsorbs more strongly than low alcohols [28], the increase of the eluting power of the eluent due to the increasing amounts of acetonitrile with respect to the fairly constant attraction by the solvated stationary phase is less pronounced than in the case of increasing methanol concentrations.

The second conclusion drawn from comparative analysis of the data collected in Table 4 is that buffering of eluents has no pronounced effect on the retention parameters considered. This would mean that the columns studied are good. According to Engelhardt et al. [29] “good means that the column provided peak symmetry for the basic solutes, and the column’s relative retention of the neutral components remained unaffected whether we used pure water or 1 mM phosphate buffer (pH 7)”. Perhaps

in the case of some stationary phases (Poly, All, TPW and XC18) there is a trend towards a decreasing $\log k_w$ after adding buffer to the eluent, but the differences observed in Table 4 may not be conclusive.

The $\log k_w$ data from 42 RP-HPLC systems, which are collected in Table 4, were subjected to principal components analysis (PCA). The first two principal components cumulatively accounted for 99.26% of total data variance. The inputs by individual chromatographic systems to these principal components’ weights (“loadings”) are plotted in Fig. 1.

Clear separation of RP-HPLC systems is observed in Fig. 1. The systems employing methanol as an organic modifier are grouped in cluster a. The systems employing acetonitrile are in cluster b, with an exception for the Alu column for the acetonitrile–water (system 36) and acetonitrile–buffer (system 38) eluents. The latter two systems evidently differ from the remaining acetonitrile systems. Since many of the test compounds have aromatic rings, this can

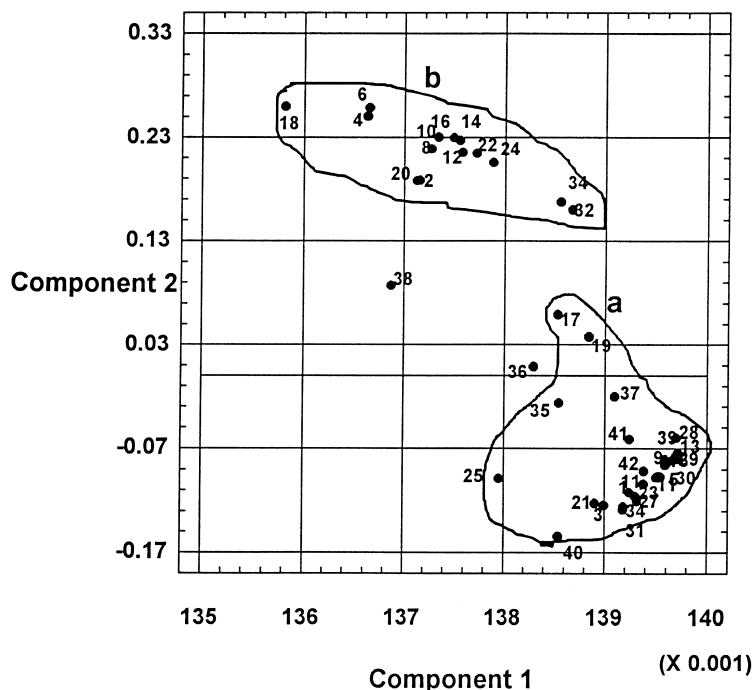


Fig. 1. Plot of first two component weights resulting from principal component analysis of $\log k_w$ data determined in all the RP-HPLC systems listed and accordingly numbered in Table 4.

be attributed to specific interactions between π -electrons of these compounds and the Lewis acidic sites present at the alumina column substrates.

The $\log k_w$ determined in the acetonitrile systems are highly mutually intercorrelated. The intercorrelations among the $\log k_w$ values originating from RP-HPLC systems employing methanol as an organic modifier are also high. The correlations of the corresponding $\log k_w$ values from the methanol against those from the acetonitrile-modified eluent systems are evidently lower.

Results of PCA illustrated in Fig. 1 unambiguously confirm that $\log k_w$ values (i.e. the logarithms of retention factors obtained by extrapolation to a hypothetical pure water eluent of the relationship between $\log k$ and the percent of organic modifier in the eluent) depend more on the organic modifier than on the properties of individual hydrocarbon-silica stationary phases. This observation does not devalue the advantage of the $\log k_w$ in QSRR analysis and in other column comparisons over the isocratic $\log k$. Even if the actual physical meaning of $\log k_w$ is

disputable [30,31], it still remains the best means of “standardizing” [32] retention parameters.

The differences among the stationary phases might be of secondary importance for the $\log k_w$ distribution patterns of test analytes as compared to the differences due to the organic modifier of the eluent. With this in mind we subjected the $\log k_w$ data obtained on individual columns with the same eluent system to PCA. In Fig. 2 the inputs by individual phases to the first two principal component weights (accounting for 99.65% of total data variance) are plotted. The results only concern the $\log k_w$ data determined for the columns studied in methanol–water eluent systems. One can note a close similarity in retention behavior of 11 stationary phases forming a compact cluster (Puro, Hyper, Sym18, Poly, NuC18, Krom, All, TTS, XC8, SeCB and Nova). Similar to those are also NuC8, XC18 and RX. The non-silica-based columns TPW and Alu exhibit totally distinct properties. The columns Sym8 and HyPuR evidently differ from the majority of the hydrocarbon-silica columns too.

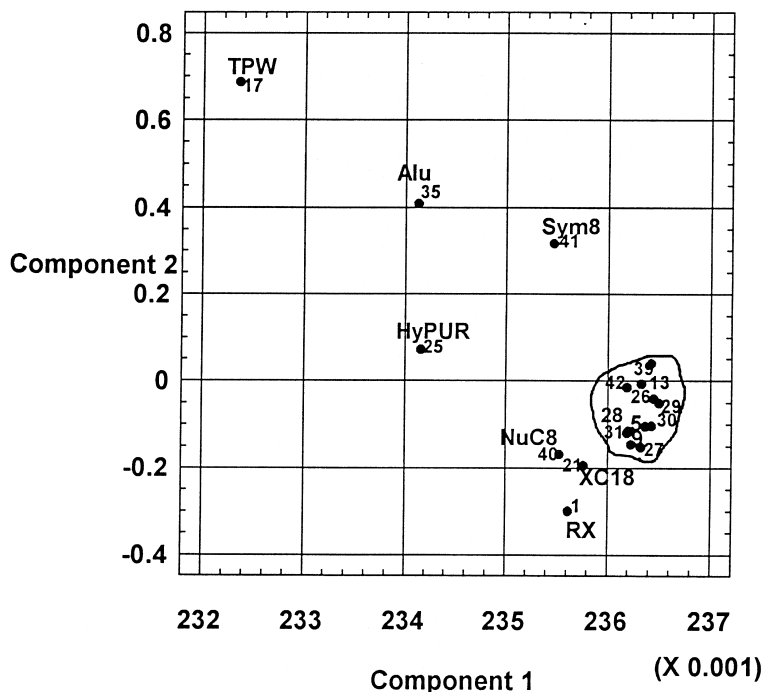


Fig. 2. Plot of first two component weights resulting from principal component analysis of $\log k_w$ data determined on the 18 columns studied when using methanol–water eluents (systems 1, 5, 9, 13, 17, 21, 25–31, 35 and 39–42 from Table 4).

It was interesting to verify whether these distribution patterns agree with the differences in retention mechanisms operating on individual columns as revealed by QSRR equations describing $\log k_w$ in terms of structural descriptors of analytes.

The $\log k_w$ data determined in this work were linearly regressed against $\log P$. The coefficients k_1 and k_2 (\pm standard deviations) of regression equations of a general form:

$$\log k_w = k_1 + k_2 \log P \quad (2)$$

are listed in Table 6 along with the numbers of data points used to derive regression (n), correlation coefficients (R), standard errors of estimate (s) and the values of the F -test for statistical significance (F).

Table 6 shows that all the $\log k_w$ data sets correlate significantly with $\log P$. The respective correlations are better in the case of data derived from the methanol–water systems than in the case of acetonitrile–water systems (higher R and F values, with lower s values). The high $\log k_w$ vs. $\log P$ correlations confirm the general similarity of the slow-equilibrium “shake-flask” octanol–water partition system and the fast-equilibrium partition chromatographic systems. If one assumes the correlation coefficients, R , from Table 6 as a measure of similarity of the overall partition mechanism operating in individual RP-HPLC systems to that determining $\log P$, then the stationary phases tested with methanol–water eluents can be ordered as follows according to their decreasing R : Sym8 > Alu > Nova \geq XC8 > TWP > Krom > Hyper \geq TTS > Sym18 \geq Puro \geq SelB \geq Poly \geq NuC18 \geq XC18 > NuC8 \geq HyPUR \geq All > RX. Such a measure of similarity may be misleading, however, because the overall correlation coefficient, R , can be affected by single outliers.

An observation drawn from Table 6 is that slopes (k_2) in Eq. (2) are evidently higher in the case of $\log k_w$ data determined with methanol as the eluent modifier than with acetonitrile. This is observed for each column for both non-buffered and buffered eluents. (As a matter of fact differences in statistical quality of Eq. (2) for buffered and non-buffered systems are insignificant.) Differences in k_2 illustrate a stronger dependence of retention on a given column for solute hydrophobicity ($\log P$) in the case

of methanolic eluents as compared to the acetonitrile-modified eluents.

The k_2 values in Table 6 are less than unity. In 1987 first Dill [33] and later Knox and Ross [34] reported that k_2 or the gradient $d(\log k)/d(\log P)$ reflects the degree to which the analyte is surrounded by the stationary phase. Accordingly, for a bonded stationary phase this should be somewhat less than for liquid octanol, so that the partitioning into the bonded phase is likely to be less with a bonded phase than with octanol – and the gradient less. Knox and Ross [34] conclude that even with pure water eluent, the gradient $d(\log k)/d(\log P)$ for C₁₈-silica phases is less than unity.

According to the above way of thinking, the more alike to octanol the solvated stationary phase is, the closer to 1 should k_2 be in Eq. (2). Taking the above into account and considering the methanol–water systems, the stationary phases can be ordered by their decreasing ability to mimic *n*-octanol as in Fig. 3. In sum, from Fig. 3 and Table 6 the most hydrophobic or lipophilic (in $\log P$ terms) columns appear to be Alu, All and Puro. The least lipophilic are NuC8 and SelB. Contrary to suggestions of other workers [29] it should be mentioned here that column hydrophobicity is not a simple function of the carbon content of a stationary phase material. Note that the Alu, All and Puro columns do not possess the highest and NuC8 and SelB the lowest carbon content of the investigated column set (see Tables 2 and 3).

Analogous ordering of phases based on the k_2 from acetonitrile–water systems generally confirms the trend, although, obviously, the acetonitrile-solvated hydrocarbonaceous stationary phases are less similar to octanol than the methanol-solvated phases. Significantly lower k_2 values than in the case of methanol–water systems are due to a stronger adsorption of acetonitrile and a higher affinity of analytes to the acetonitrile-solvated hydrocarbon of the stationary phase.

Hydrophobicity parameters of the stationary phases provided by QSRRs can be discussed in relation to the results of the standard empirical column tests performed independently. On the same set of columns Claessens et al. [35] performed a comparative study of several test methods reported in the literature [36–40]. It was found that none of the

Table 6

Regression coefficients (\pm standard deviations), numbers of data points used to derive regression (n), correlation coefficients (R), standard errors of estimate (s) and F -test values (F) of regression equations $\log k_w = k_1 + k_2 \log P$

Chromatographic system	k_1	k_2	n	R	s	F
<i>C₁₈ columns</i>						
RX						
(MeOH–water)	0.3081 (± 0.1165)	0.8033 (± 0.0425)	21	0.9745	0.2891	358
(ACN–water)	0.0136 (± 0.1477)	0.6371 (± 0.0545)	22	0.9339	0.3719	136
(MeOH–buffer)	0.2720 (± 0.1217)	0.8296 (± 0.0454)	23	0.9699	0.3103	334
(ACN–buffer)	-0.0250 (± 0.1231)	0.6434 (± 0.0460)	23	0.9504	0.3140	196
Hyper						
(MeOH–water)	0.2107 (± 0.0865)	0.8136 (± 0.0315)	21	0.9860	0.2146	666
(ACN–water)	-0.0763 (± 0.1111)	0.6550 (± 0.0405)	21	0.9655	0.2757	262
(MeOH–buffer)	0.2169 (± 0.0808)	0.8159 (± 0.0302)	23	0.9860	0.2060	732
(ACN–buffer)	-0.0439 (± 0.1044)	0.6312 (± 0.0390)	23	0.9622	0.2662	262
Poly						
(MeOH–water)	0.3860 (± 0.0944)	0.8068 (± 0.0344)	21	0.9832	0.2342	550
(ACN–water)	0.0212 (± 0.1088)	0.6470 (± 0.0397)	21	0.9661	0.2701	266
(MeOH–buffer)	0.3525 (± 0.0931)	0.7928 (± 0.0348)	23	0.9804	0.2375	520
(ACN–buffer)	-0.0430 (± 0.1066)	0.6389 (± 0.0398)	23	0.9616	0.2719	258
All						
(MeOH–water)	0.3202 (± 0.1140)	0.8553 (± 0.0421)	22	0.9766	0.287	413
(ACN–water)	0.1159 (± 0.1557)	0.6676 (± 0.0581)	23	0.9288	0.3970	132
(MeOH–buffer)	0.4361 (± 0.0798)	0.8206 (± 0.0298)	23	0.9864	0.2035	759
(ACN–buffer)	0.2002 (± 0.1084)	0.6515 (± 0.0405)	23	0.9618	0.2765	259
TPW						
(MeOH–water)	0.2646 (± 0.0700)	0.7874 (± 0.0255)	21	0.9902	0.1736	953
(ACN–water)	0.3010 (± 0.0924)	0.5428 (± 0.0337)	21	0.9653	0.2294	259
(MeOH–buffer)	0.2480 (± 0.0633)	0.7838 (± 0.0236)	23	0.9906	0.1615	1099
(ACN–buffer)	0.3271 (± 0.0956)	0.5226 (± 0.0357)	23	0.9544	0.2437	215
XC18						
(MeOH–water)	0.4457 (± 0.0977)	0.7839 (± 0.0356)	21	0.9810	0.2424	484
(ACN–water)	-0.0175 (± 0.1110)	0.6632 (± 0.0405)	21	0.9664	0.2756	268
(MeOH–buffer)	0.3296 (± 0.0961)	0.8186 (± 0.0359)	23	0.9804	0.2450	521
(ACN–buffer)	-0.0921 (± 0.1119)	0.6754 (± 0.0418)	23	0.9621	0.2855	261

Table 6. (Continued)

Chromatographic system	k_1	k_2	n	R	s	F
HyPUR (MeOH–water)	0.0304	0.7952	21	0.9777	0.2667	412
<i>C₁₈ columns</i>	(±0.1075)	(±0.0392)				
Krom (MeOH–water)	0.3928 (±0.0770)	0.8121 (±0.0281)	21	0.9888	0.1910	837
NuC18 (MeOH–water)	0.3769 (±0.0937)	0.7865 (±0.0342)	21	0.9826	0.2325	530
Puro (MeOH–water)	0.3250 (±0.0951)	0.8376 (±0.0347)	21	0.9841	0.2360	584
Sym18 (MeOH–water)	0.4079 (±0.0834)	0.8061 (±0.0312)	23	0.9847	0.2128	669
TTS (MeOH–water)	0.3665 (±0.0848)	0.7904 (±0.0309)	21	0.9858	0.2106	653
<i>C₈ columns</i>						
SelB (MeOH–water)	0.2592 (±0.0843)	0.7274 (±0.0307)	21	0.9835	0.2092	560
(ACN–water)	0.1231 (±0.0819)	0.5847 (±0.0298)	21	0.9761	0.2032	384
(MeOH–buffer)	0.2996 (±0.0757)	0.7089 (±0.0282)	23	0.9837	0.1930	630
(ACN–buffer)	0.0920 (±0.0883)	0.5900 (±0.0330)	23	0.9687	0.2253	320
Alu (MeOH–water)	–0.7757 (±0.0602)	0.8741 (±0.0219)	21	0.9941	0.1493	1588
(ACN–water)	–0.4789 (±0.0682)	0.6579 (±0.0248)	21	0.9867	0.1693	700
(MeOH–buffer)	–0.6767 (±0.0808)	0.8368 (±0.0295)	22	0.9878	0.1830	804
(ACN–buffer)	–0.5620 (±0.0793)	0.6342 (±0.0296)	23	0.9778	0.2024	458
Nova (MeOH–water)	0.3242 (±0.0590)	0.7574 (±0.0215)	21	0.9924	0.1464	1240
NuC8 (MeOH–water)	0.2812 (±0.0822)	0.6268 (±0.0300)	21	0.9789	0.2041	437
Sym8 (MeOH–water)	0.2054 (±0.0437)	0.7582 (±0.0159)	21	0.9958	0.1084	2268
XC8 (MeOH–water)	0.3426 (±0.0618)	0.7781 (±0.0225)	21	0.9921	0.1533	1194

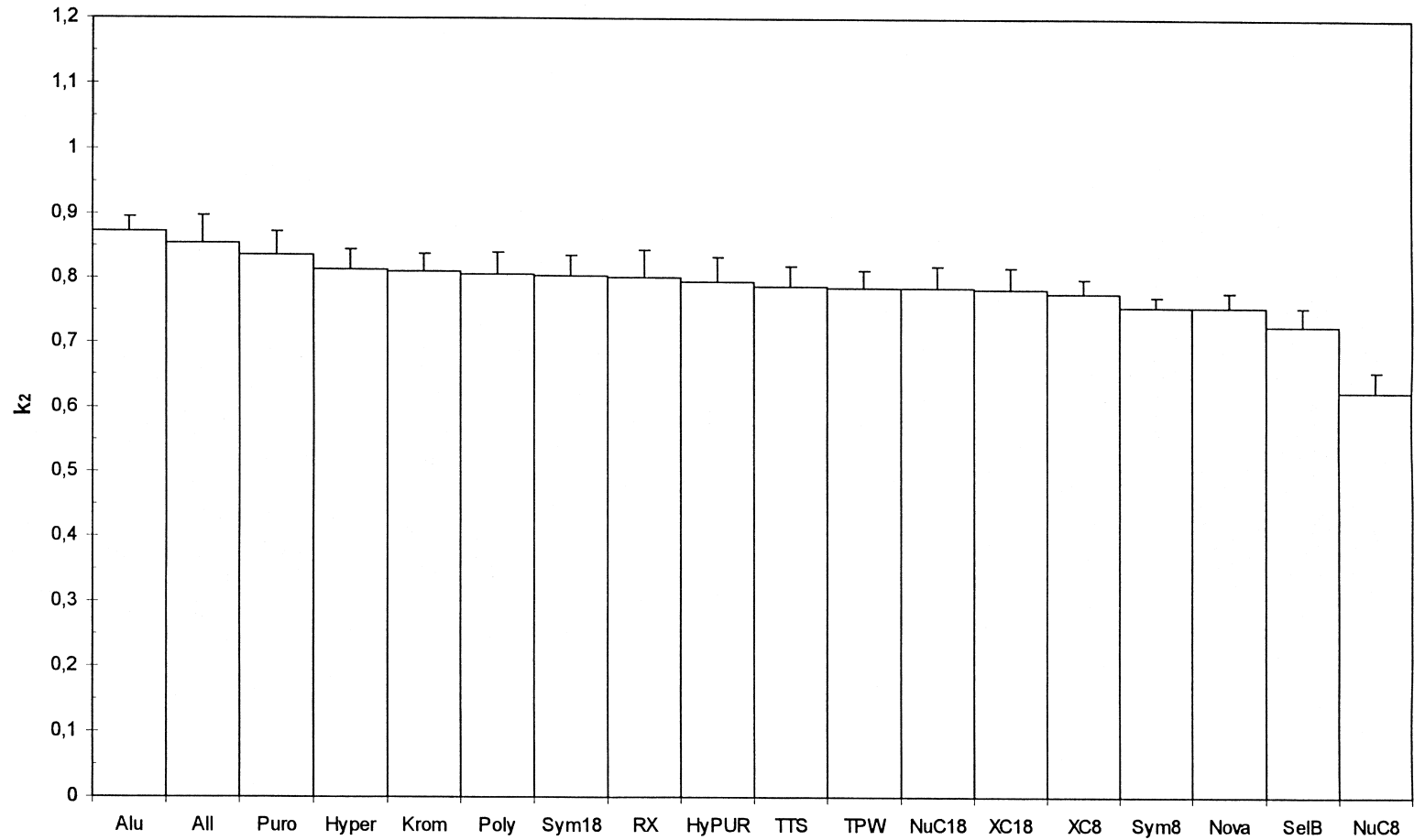


Fig. 3. Slopes (k_2 values from Table 6) of the $\log k_w$ vs. $\log P$ relationship for the 18 columns tested. The $\log k_w$ data considered were determined in methanol–water eluent systems.

recommended hydrophobicity tests were able to differentiate between the silica-based reversed-phase materials studied.

The authors of the standard testing methods [36–40] considered some hydrocarbon selectivity parameters as a measure of hydrophobicity, e.g., $k_{\text{anthracene}}/k_{\text{benzene}}$ [36], $k_{\text{amylbenzene}}/k_{\text{butylbenzene}}$ [37] or $k_{\text{ethylbenzene}}/k_{\text{toluene}}$ [38]. Evidently, such a measure of stationary phase properties is inappropriate for comparisons of hydrocarbon-bound silica columns.

Hydrophobicity (lipophilicity) is a complex net effect of various competing intermolecular interactions of an analyte placed in a two-phase water–organic system in which the molecules form its environment. Two basic kinds of attractive intermolecular interactions must be taken into consideration: the chemically non-specific, molecularly-sized or bulkiness-related, dispersive (London-type) interactions and the polar interactions more or less dependent on chemical constitution (inductive, orientation, hydrogen-bonding and charge-transfer interactions). Using test hydrocarbon analytes the empirical tests [36–40] can provide some information about the non-specific dispersive retentivity of the stationary phases studied but not about their hydrophobicity. The former especially concerns the procedures employing $\log k$ data of aromatic hydrocarbons aimed at the determination of the amount of alkyl chains in stationary phase-materials [37], the size selectivity of the columns [39] and the phase hydrophobicity (an alternative method) [36]. The following QSRR analysis confirms this assumption.

In Table 7 the results are given of a multiple regression analysis of $\log k_w$ data from Table 4 in terms of Abraham's LSER-based parameters of test analytes collected in Table 5. The parameters considered are not intercorrelated: the highest is the correlation between π_2^H and β_2^H ($R=0.606$). Full Abraham equations have a good predictive power regarding retention. Several authors [9,11] have used such full equations for the comparison of several hydrocarbon-silica columns. However, in our case, relatively high standard deviations of some regression coefficients proved the lack of statistical significance in QSRR equations of some LSER-based parameters of analytes. For that reason we modified the general Abraham's equation retaining only the terms significant above the 95% significance level. The results are given in Table 7.

For every set of investigated $\log k_w$ data the most significant ones for retention appeared to be the hydrogen-bond basicity (β_2^H) and McGowan volume (V_x) of analytes. These parameters are often reported as affecting retention most in RP-HPLC [1,8]. The third significant analyte parameter in LSER-based QSRR is either dipolarity/polarizability (π_2^H) in the case of methanolic eluents or hydrogen-bond acidity (α_2^H) in the case of acetonitrile-modified mobile phases. In the case of methanol–water systems, α_2^H is highly significant in QSRR for All and Puro columns and less significant for RX and Poly columns. For the Alu column the excess molar refraction (R_2) also appeared to be significant.

The equations presented in Table 7 make good physical sense. Coefficient k'_6 with the McGowan volume term is positive. We interpret that the attractive dispersive interactions between the analyte and the bulky hydrocarbon ligand of the stationary phase are stronger than the same non-specific attractive interactions between the analyte and the small molecules (water, acetonitrile, and methanol) of the eluent. The net effect of attractive interactions of a hydrogen-bond acceptor analyte with non-polar stationary phase, on one hand, and with the polar components of the eluent, which is an efficient hydrogen-bond donor, on the other hand, are obviously negative. This is confirmed by the negative sign at k'_5 .

The term reflecting solute dipolarity/polarizability (π_2^H) is always significant, if methanol is used to derive $\log k_w$. Its negative sign reflects the higher strength of dipole–dipole and dipole–induced dipole attractive interactions between the solute and the polar molecules of the eluent as compared to the same type of interactions between the analyte and the non-polar stationary phase (even if solvated).

If acetonitrile is used to determine $\log k_w$, the respective LSER-based QSRR equations usually comprise the hydrogen-bond acidity term (α_2^H) instead of π_2^H . Again, the sign is negative as expected, because the hydrogen-bonding of analyte with the polar eluent serving as a hydrogen-bond acceptor is stronger than with the hydrocarbonaceous stationary phase.

The differences in retention mechanisms in RP-HPLC systems employing methanol and acetonitrile as the components of eluents, which manifest themselves in QSRR equations in Table 7, can be

Table 7

Regression coefficients (\pm standard deviations), numbers of data points used to derive regression (n), correlation coefficients (R), standard errors of estimate (s) and F -test values (F) of regression equations $\log k_w = k'_1 + k'_2 R_2 + k'_3 \pi_2^H + k'_4 \alpha_2^H + k'_5 \beta_2^H + k'_6 V_x$

Chromatographic system	k'_1	k'_2	k'_3	k'_4	k'_5	k'_6	n	R	s	F
<i>C₁₈ columns</i>										
RX										
(MeOH–water)	0.3071 (± 0.2869)		-0.6327 (± 0.2118)	-0.5181 (± 0.2155)	-2.4120 (± 0.2575)	3.4272 (± 0.1906)	23	0.9874	0.2690	176
(ACN–water)	0.6561 (± 0.1938)			-0.9599 (± 0.1463)	-2.8535 (± 0.1511)	2.0252 (± 0.1530)	24	0.9847	0.2179	213
(MeOH–buffer)	0.3207 (± 0.2889)		-0.6143 (± 0.2036)	-0.5976 (± 0.1967)	-2.4793 (± 0.2445)	3.4652 (± 0.1931)	25	0.9863	0.2739	179
(ACN–buffer)	0.7306 (± 0.1447)			-0.9547 (± 0.1063)	-2.8174 (± 0.1120)	1.9284 (± 0.1148)	25	0.9905	0.1645	364
Hyper										
(MeOH–water)	0.3034 (± 0.2567)		-0.8402 (± 0.1630)		-2.3094 (± 0.2028)	3.4080 (± 0.1679)	23	0.9892	0.2411	288
(ACN–water)	0.6779 (± 0.1496)			-0.8097 (± 0.1157)	-2.9599 (± 0.1172)	1.9346 (± 0.1181)	23	0.9909	0.1680	345
(MeOH–buffer)	0.2831 (± 0.2348)		-0.8375 (± 0.1500)		-2.3385 (± 0.1851)	3.4371 (± 0.1549)	25	0.9899	0.2240	342
(ACN–buffer)	0.5472 (± 0.1678)			-0.7310 (± 0.1234)	-2.7157 (± 0.1300)	1.9658 (± 0.1331)	25	0.9864	0.1908	252
Poly										
(MeOH–water)	0.5902 (± 0.2575)		-0.6516 (± 0.1901)	-0.4529 (± 0.1934)	-2.4994 (± 0.2311)	3.2599 (± 0.1710)	23	0.9895	0.2414	211
(ACN–water)	0.7186 (± 0.1433)			-0.8906 (± 0.1109)	-2.8307 (± 0.1123)	1.9428 (± 0.1132)	23	0.9913	0.1611	361
(MeOH–buffer)	0.4237 (± 0.2284)		-0.6690 (± 0.1609)	-0.4065 (± 0.1555)	-2.3730 (± 0.1933)	3.3303 (± 0.1526)	25	0.9907	0.2165	265
(ACN–buffer)	0.6207 (± 0.1402)			-0.8672 (± 0.1031)	-2.7259 (± 0.1086)	1.9499 (± 0.1112)	25	0.9907	0.1590	370
All										
(MeOH–water)	0.4657 (± 0.2761)		-0.5150 (± 0.1983)	-0.5620 (± 0.1987)	-2.8494 (± 0.2424)	3.4395 (± 0.1852)	24	0.9885	0.2618	203
(ACN–water)	0.9938 (± 0.2085)			-1.0127 (± 0.1532)	-2.9942 (± 0.1614)	1.9384 (± 0.1654)	25	0.9822	0.2370	191
(MeOH–buffer)	0.6008 (± 0.2024)		-0.6811 (± 0.1427)	-0.3860 (± 0.1378)	-2.5429 (± 0.1713)	3.3665 (± 0.1353)	25	0.9930	0.1920	356
(ACN–buffer)	1.0884 (± 0.1587)		-0.2536 (± 0.1118)	-0.6966 (± 0.1080)	-2.6413 (± 0.1343)	1.9407 (± 0.1060)	25	0.9924	0.1504	327
TPW										
(MeOH–water)	0.5177 (± 0.1938)		-0.2800 (± 0.1230)		-2.9580 (± 0.1530)	2.8104 (± 0.1267)	23	0.9924	0.1820	412
(ACN–water)	0.8526 (± 0.1660)			-0.3514 (± 0.1284)	-2.3532 (± 0.1301)	1.5460 (± 0.1311)	23	0.9819	0.1867	170
(MeOH–buffer)	0.4108 (± 0.1752)		-0.2936 (± 0.1119)		-2.8886 (± 0.1381)	2.8851 (± 0.1156)	25	0.9930	0.1672	498
(ACN–buffer)	0.6374 (± 0.1878)			-0.3364 (± 0.1380)	-2.2169 (± 0.1454)	1.7170 (± 0.1490)	25	0.9750	0.2135	134
XC18										
(MeOH–water)	0.4744 (± 0.2566)		-0.9344 (± 0.1630)		-2.0829 (± 0.2027)	3.4328 (± 0.1678)	23	0.9890	0.2410	284
(ACN–water)	0.6344 (± 0.1535)			-0.8655 (± 0.1188)	-2.9096 (± 0.1203)	2.0464 (± 0.1212)	23	0.9907	0.1726	336
(MeOH–buffer)	0.3275 (± 0.2725)		-0.8800 (± 0.1741)		-2.2569 (± 0.2147)	3.5276 (± 0.1798)	25	0.9868	0.2601	260
(ACN–buffer)	0.5770 (± 0.1421)			-0.8961 (± 0.1045)	-2.9168 (± 0.1100)	2.1037 (± 0.1127)	25	0.9916	0.1616	412

Table 7. (Continued)

Chromatographic system	k'_1	k'_2	k'_3	k'_4	k'_5	k'_6	n	R	s	F
HyPUR (MeOH–water)	0.2161		–0.7692		–2.3284	3.2039	23	0.9791	0.3232	147
<i>C₁₈ columns</i>	(±0.3441)		(±0.2185)		(±0.2718)	(±0.2250)				
Krom (MeOH–water)	0.5899 (±0.2405)		–0.8450 (±0.1527)		–2.3353 (±0.1900)	3.3125 (±0.1573)	23	0.9903	0.2259	321
NuC18 (MeOH–water)	0.3842 (±0.2585)		–0.8233 (±0.1641)		–2.1537 (±0.2042)	3.3594 (±0.1690)	23	0.9884	0.2428	267
Puro (MeOH–water)	0.6564 (±0.2398)		–0.7029 (±0.1770)	–0.5024 (±0.1801)	–2.6098 (±0.2153)	3.3056 (±0.1593)	23	0.9914	0.2248	260
Sym18 (MeOH–water)	0.5738 (±0.2433)		–0.8594 (±0.1554)		–2.2829 (±0.1918)	3.3159 (±0.1605)	25	0.9887	0.2323	304
TTS (MeOH–water)	0.4264 (±0.2400)		–0.8134 (±0.1524)		–2.2239 (±0.1896)	3.3288 (±0.1570)	23	0.9900	0.2255	311
<i>C₈ columns</i>										
SeIB (MeOH–water)	0.1300 (±0.2395)		–0.6312 (±0.1521)		–2.0788 (±0.1892)	3.1335 (±0.1566)	23	0.9881	0.2249	262
(ACN–water)	0.5246 (±0.1239)			–0.6797 (±0.0958)	–2.4705 (±0.0971)	1.9228 (±0.0978)	23	0.9921	0.1393	398
(MeOH–buffer)	0.1677 (±0.2270)		–0.5772 (±0.1450)		–2.0835 (±0.1789)	3.0322 (±0.1498)	25	0.9872	0.2167	269
(ACN–buffer)	0.5323 (±0.1227)			–0.7024 (±0.0902)	–2.5291 (±0.0950)	1.9565 (±0.0973)	25	0.9920	0.1394	432
Alu										
(MeOH–water)	–0.5664 (±0.2961)	0.6056 (±0.2086)	–0.8036 (±0.2475)		–2.6940 (±0.2458)	2.9541 (±0.2123)	23	0.9862	0.2743	159
(ACN–water)	–0.1472 (±0.2143)	0.5773 (±0.1509)	–0.7675 (±0.1791)		–2.0622 (±0.1778)	2.1329 (±0.1536)	23	0.9879	0.1984	182
(MeOH–buffer)	–0.3781 (±0.2246)	0.7988 (±0.1735)	–1.1094 (±0.1956)		–2.5800 (±0.1918)	2.8586 (±0.1627)	24	0.9896	0.2114	225
(ACN–buffer)	–0.1148 (±0.2403)	0.7336 (±0.1715)	–0.7967 (±0.2022)		–1.9089 (±0.1985)	1.7855 (±0.1740)	25	0.9796	0.2262	119
Nova (MeOH–water)	0.4030 (±0.2140)		–0.6525 (±0.1359)		–2.2913 (±0.1690)	3.0889 (±0.1399)	23	0.9910	0.2010	346
NuC8 (MeOH–water)	–0.0122 (±0.2144)		–0.4852 (±0.1362)		–1.8035 (±0.1694)	2.8275 (±0.1402)	23	0.9876	0.2014	251
Sym8 (MeOH–water)	0.2856 (±0.1978)		–0.4766 (±0.1256)		–2.5275 (±0.1562)	2.9831 (±0.1294)	23	0.9920	0.1858	392
XC8 (MeOH–water)	0.5104 (±0.1982)		–0.8119 (±0.1259)		–2.3134 (±0.1566)	3.2296 (±0.1296)	23	0.9931	0.1862	452

Table 8

Regression coefficients (\pm standard deviations), numbers of data points used to derive regression (n), correlation coefficients (R), standard errors of estimate (s) and F -test values (F) of regression equations $\log k_w = k_1'' + k_2'' \delta_{\min} + k_3'' \mu^2 + k_4'' \text{SAS}$

Chromatographic system	k_1''	k_2''	k_3''	k_4''	n	R	s	F
<i>C₁₈ columns</i>								
RX								
(MeOH–water)	–1.9537 (± 0.5862)	5.1076 (± 1.2992)	–0.1027 (± 0.0237)	0.0191 (± 0.0017)	23	0.9646	0.4371	85
(ACN–water)	–0.2318 (± 0.5572)	4.8944 (± 1.1726)	–0.0975 (± 0.0223)	0.0110 (± 0.0016)	24	0.9431	0.4154	54
(MeOH–buffer)	–2.0716 (± 0.5948)	4.6428 (± 1.2612)	–0.1027 (± 0.0234)	0.0194 (± 0.0017)	25	0.9611	0.4478	85
(ACN–buffer)	–0.2324 (± 0.5545)	3.9734 (± 1.1758)	–0.1043 (± 0.0218)	0.0104 (± 0.0016)	25	0.9373	0.4171	51
Hyper								
(MeOH–water)	–1.7584 (± 0.6068)	5.2234 (± 1.3450)	–0.1064 (± 0.0245)	0.0184 (± 0.0018)	23	0.9614	0.4524	77
(ACN–water)	–0.1280 (± 0.5948)	3.8828 (± 1.3182)	–0.1191 (± 0.0240)	0.0099 (± 0.0017)	23	0.9352	0.4434	44
(MeOH–buffer)	–1.8920 (± 0.6272)	4.6141 (± 1.3299)	–0.1020 (± 0.0246)	0.0185 (± 0.0018)	25	0.9545	0.4721	72
(ACN–buffer)	–0.4063 (± 0.5639)	3.4053 (± 1.1958)	–0.1032 (± 0.0222)	0.0103 (± 0.0016)	25	0.9307	0.4245	45
Poly								
(MeOH–water)	–1.4944 (± 0.5919)	5.3173 (± 1.3118)	–0.1049 (± 0.0239)	0.0181 (± 0.0017)	23	0.9625	0.4413	80
(ACN–water)	–0.1372 (± 0.5337)	4.0718 (± 1.1830)	–0.1116 (± 0.0216)	0.0102 (± 0.0015)	23	0.9460	0.3979	54
(MeOH–buffer)	–1.8490 (± 0.5794)	4.5562 (± 1.2286)	–0.0970 (± 0.0228)	0.0185 (± 0.0017)	25	0.9597	0.4361	82
(ACN–buffer)	–0.3226 (± 0.4952)	3.7290 (± 1.0500)	–0.1046 (± 0.0194)	0.0104 (± 0.0014)	25	0.9479	0.3728	62
All								
(MeOH–water)	–1.5191 (± 0.6105)	5.4318 (± 1.2849)	–0.1147 (± 0.0245)	0.0186 (± 0.0018)	24	0.9629	0.4553	85
(ACN–water)	0.1284 (± 0.5214)	4.3827 (± 1.1056)	–0.1156 (± 0.0205)	0.0104 (± 0.0015)	25	0.9503	0.3925	65
(MeOH–buffer)	–1.6649 (± 0.6287)	4.4885 (± 1.3331)	–0.1066 (± 0.0247)	0.0185 (± 0.0018)	25	0.9548	0.4733	72
(ACN–buffer)	–0.0146 (± 0.5278)	3.8413 (± 1.1192)	–0.1071 (± 0.0207)	0.0104 (± 0.0015)	25	0.9432	0.3974	56
TPW								
(MeOH–water)	–0.5592 (± 0.6892)	3.9018 (± 1.5274)	–0.1315 (± 0.0278)	0.0137 (± 0.0020)	23	0.9378	0.5139	46
(ACN–water)	0.4498 (± 0.4632)	2.9622 (± 1.0267)	–0.0997 (± 0.0187)	0.0074 (± 0.0013)	23	0.9367	0.3454	45
(MeOH–buffer)	–0.8739 (± 0.6757)	3.3637 (± 1.4327)	–0.1223 (± 0.0265)	0.0142 (± 0.0020)	25	0.9338	0.5087	48
(ACN–buffer)	0.0235 (± 0.4373)	2.6480 (± 0.9272)	–0.0901 (± 0.0172)	0.0085 (± 0.0013)	25	0.9394	0.3292	52
XC18								
(MeOH–water)	–1.8512 (± 0.6002)	4.5353 (± 1.3302)	–0.1074 (± 0.0242)	0.0187 (± 0.0017)	23	0.9617	0.4475	78
(ACN–water)	–0.2461 (± 0.5380)	4.2919 (± 1.1923)	–0.1130 (± 0.0217)	0.0108 (± 0.0016)	23	0.9487	0.4011	57
(MeOH–buffer)	–1.9430 (± 0.5809)	4.5094 (± 1.2317)	–0.1059 (± 0.0228)	0.0190 (± 0.0017)	25	0.9622	0.4373	87
(ACN–buffer)	–0.4256 (± 0.5328)	4.1635 (± 1.1297)	–0.1077 (± 0.0209)	0.0113 (± 0.0015)	25	0.9472	0.4011	61

Table 8. (Continued)

Chromatographic system	k''_1	k''_2	k''_3	k''_4	n	R	s	F
HyPUR (MeOH–water)	–1.8083	3.0315	–0.1382	0.0165	23	0.9495	0.4989	58
<i>C₁₈ columns</i>	(±0.6690)	(±1.4828)	(±0.0270)	(±0.0019)				
Krom (MeOH–water)	–1.4573 (±0.6346)	4.8689 (1.4064)	–0.1118 (±0.0256)	0.0178 (±0.0018)	23	0.9566	0.4732	68
NuC18 (MeOH–water)	–1.7047 (±0.5724)	4.8219 (±1.2687)	–0.1028 (±0.0231)	0.0182 (±0.0016)	23	0.9635	0.4268	82
Puro (MeOH–water)	–1.5077 (±0.6267)	5.3904 (±1.3890)	–0.1129 (±0.0253)	0.0183 (±0.0018)	23	0.9604	0.4673	75
Sym18 (MeOH–water)	–1.6739 (±0.6946)	4.0857 (±1.4728)	–0.1027 (±0.0273)	0.0179 (±0.0020)	25	0.9413	0.5229	54
TTS (MeOH–water)	–1.6242 (±0.5936)	4.8520 (±1.3157)	–0.1044 (±0.0240)	0.0179 (±0.0017)	23	0.9608	0.4426	76
<i>C₈ columns</i>								
SelB (MeOH–water)	–1.6623 (±0.5416)	4.7467 (±1.2004)	–0.0863 (±0.0219)	0.0169 (±0.0016)	23	0.9612	0.4038	77
(ACN–water)	–0.3104 (±0.4651)	3.6996 (±1.0309)	–0.0937 (±0.0188)	0.0101 (±0.0013)	23	0.9502	0.3468	59
(MeOH–buffer)	–1.5785 (±0.5281)	4.0924 (±1.1198)	–0.0831 (±0.0207)	0.0162 (±0.0015)	25	0.9564	0.3975	75
(ACN–buffer)	–0.3704 (±0.4561)	3.5558 (±0.9671)	–0.0938 (±0.0179)	0.0104 (±0.0013)	25	0.9504	0.3433	65
Alu (MeOH–water)	–2.0056 (±0.7274)	4.7425 (±1.6122)	–0.1237 (±0.0294)	0.0162 (±0.0021)	23	0.9416	0.5424	49
(ACN–water)	–1.1937 (±0.5362)	3.9673 (±1.1885)	–0.0997 (±0.0217)	0.0119 (±0.0016)	23	0.9469	0.3998	55
(MeOH–buffer)	–2.0203 (±0.6795)	4.4968 (±1.4425)	–0.1011 (±0.0275)	0.0160 (±0.0020)	24	0.9344	0.5111	46
(ACN–buffer)	–1.0202 (±0.5208)	3.1816 (±1.1042)	–0.0943 (±0.0204)	0.0103 (±0.0015)	25	0.9341	0.3920	48
Nova (MeOH–water)	–1.3633 (±0.6060)	4.5518 (±1.3432)	–0.1012 (±0.0245)	0.0164 (±0.0018)	23	0.9535	0.4519	63
NuC8 (MeOH–water)	–1.5699 (±0.4751)	4.2158 (±1.0530)	–0.0690 (±0.0192)	0.0152 (±0.0014)	23	0.9612	0.3543	77
Sym8 (MeOH–water)	–1.2223 (±0.6554)	4.1946 (±1.4527)	–0.1088 (±0.0265)	0.0154 (±0.0019)	23	0.9434	0.4888	51
XC8 (MeOH–water)	–1.4872 (±0.6366)	4.8171 (±1.4110)	–0.1066 (±0.0257)	0.0173 (±0.0018)	23	0.9540	0.4747	64

rationalized as follows. The dispersive interactions of analytes (characterized by V_x) and the hydrogen-bonding interactions in which the analyte molecule is a hydrogen-bond acceptor (characterised by β_2^H) significantly affect the retention of analytes in both water–methanol–stationary phase and water–acetonitrile–stationary phase equilibrium systems. However, in methanolic systems, the third significant factor determining equilibrium is the ability of the analyte molecule to be preferentially attracted by polar molecules of eluent due to dipole–dipole and dipole–induced dipole interactions (characterised by π_2^H). In the systems containing acetonitrile the π_2^H descriptor becomes insignificant in QSRR equations. What is significant is the ability of an analyte to be preferentially attracted by the eluent due to hydrogen-bonding. In that type of hydrogen-bonding the analyte serves as a donor of hydrogen, characterized by the α_2^H descriptor. In such a situation the well-known hydrogen-bond acceptor properties of acetonitrile clearly manifest themselves in QSRR equa-

tions as a retention-decreasing term $k'_4 \alpha_2^H$ with a negative value of the k'_4 regression coefficient.

QSRR equations collected in Table 7 have a definite physical sense. They distinguish some of the columns tested. Discussion of these equations will be more comprehensible, if we first analyze the QSRRs relating $\log k_w$ to simple structural parameters from molecular modeling.

In Table 8 the QSRR equations are given that describe $\log k_w$ in terms of structural descriptors of analytes readily obtained by the now commonly available computation chemistry methods. It is evident that QSRRs of quite a good statistical quality relate $\log k_w$ to the maximum atomic excess of electrons (δ_{\min}), square of total dipole moment (μ^2), and Van der Waals surface area of a molecule that is accessible to a molecule of water (SAS).

QSRR equations from Table 8 make good physical sense. These equations have a slightly lower retention predictive ability than the equations previously discussed, which employed the laboriously ac-

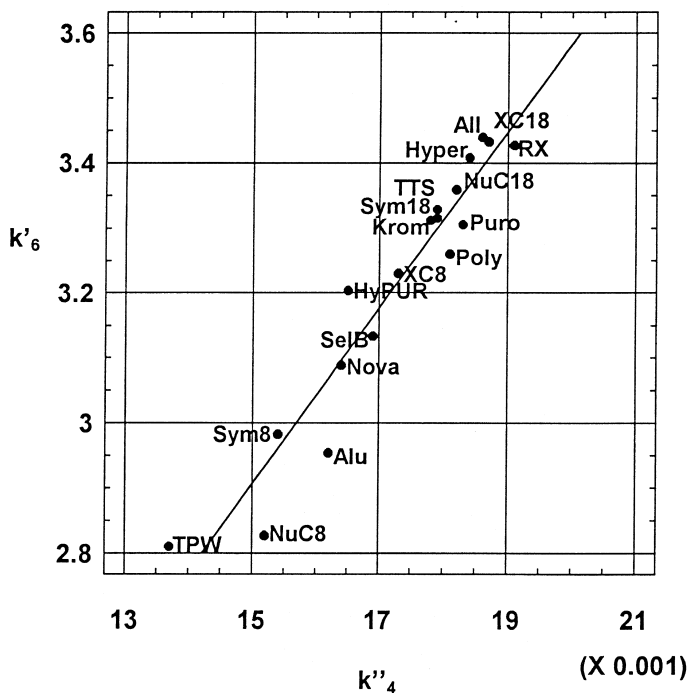


Fig. 4. Ordering of stationary phases according to their non-specific retentivity due to dispersion interactions quantified by the coefficient k'_6 for the V_x variable (Table 7) and the coefficient k''_4 for the SAS variable (Table 8) in QSRR equations employing the LSER-based and the molecular modeling-based structural descriptors of test analytes. Regression line k'_6 vs. k''_4 is drawn between the column data points.

quired empirical descriptors. As expected, the net positive effect to retention is due to the SAS parameter. This parameter is evidently related to the ability of analytes to participate in dispersive London-type interactions. These interactions are stronger between the analyte and the bulky hydrocarbon ligand of the stationary phase than between the same analyte and the small molecules of the eluent used. Hence, the k_4'' regression coefficient has a positive sign. Note that the changes in the magnitude of the regression coefficient k_4'' before SAS in the QSRR equations in Table 8 are parallel to the changes in the coefficient k_6' before V_x in the LSER equations in Table 7. There is a very high intercorrelation between the two coefficients: $R=0.9594$ (Fig. 4). This means that V_x is interchangeable with the easily calculated SAS.

We assume that the ordering of stationary phases along the k_6' vs. k_4'' regression line in Fig. 4 follows their non-specific retentivity (London retentivity). Abraham et al. [11] consider the coefficient before V_x in their equations as a measure of “intrinsic hydrophobicity” of the columns. As discussed above, hydrophobicity is a net effect of non-specific, dispersive or London intermolecular interactions and of some or all polar interactions (dipole–dipole, dipole–induced dipole, hydrogen-bonding, and electron pair donor–electron pair acceptor). The coefficients in QSRR equations, which are complementary to V_x or SAS, only account for the ability of an individual stationary phase to participate in non-polar London-type intermolecular interaction. These interactions require a close contact of interacting molecular fragments. Larger values of k_4'' and k_6' would suggest a larger surface area of the stationary phase hydrocarbon moiety accessible to the analyte molecules. Hence, the absolute hydrocarbon load of a stationary phase does not need to correlate perfectly with either k_4'' or k_6' . Based on Fig. 4 and on the numerical data from Tables 7 and 8, we assume the stationary phases All, XC18, RX, Hyper possess the most developed surface area of external hydrocarbon ligands and, hence, the highest non-specific London retentivity. At the other end we have the phases TPW, NuC8, Sym8 and Alu, which show the lowest London retentivity.

The proposed measures of non-specific dispersive retentivity of stationary phases, k_6' and k_4'' , signifi-

Table 9
Correlation matrix for the parameters of non-specific (London-type) retentivity of 18 stationary phases studied^a

<i>R</i>	k_6'	k_4''	AAC	SSG
k_4''	0.9583	1	0.8015	0.9317
AAC	0.8654	0.8015	1	0.7903
SSG	0.9407	0.9317	0.7903	1
HBH	0.9166	0.8349	0.9103	0.808

^a Parameter k_6' is the regression coefficient for the McGowan volume of analyte, V_x (Table 7); k_4'' is the regression coefficient for the water-accessible surface area of analyte, SAS (Table 8); AAC is the parameter designed [37] to account for the amount of alkyl chains in the stationary phase; SSG is the parameter designed [39] to reflect analyte size selectivity; HBH is the parameter to account for differences in hydrophobicity of stationary phases ($\log k_w$, hexylbenzene). The numerical values of AAC, SSG and HBH for correlation analysis were taken from Claessens et al. [35].

cantly correlate (Table 9) with some column parameters provided by the standard testing procedures [36–40] when selected aromatic hydrocarbons are used as probe analytes. Both k_6' and k_4'' correlate especially well with the so-called size selectivity parameter of Galushko [39] (SSG in Table 9). This is understandable because SSG is determined via the increments of partial molar volume of structural fragments of test analytes [39,41].

Mutual correlation is rather low (Table 9) between the non-specific retentivity parameters from classical tests, i.e., AAC (amount of alkyl chains according to Tanaka et al. [37]), SSG (analyte size selectivity according to Galushko [39]) and HBH (hydrophobicity expressed as $\log k_w$ calculated for hexylbenzene). The reason may be that the aromatic test analytes employed undergo some polar interactions due to their conjugated bond systems in addition to the prevailing dispersive interactions. We postulate the k_6' and k_4'' parameters are the more “pure” measures of non-specific retentivity.

It is important to emphasize here that apart from the non-specific (London-type) retention properties of RP-HPLC columns the polar properties in most cases dominantly determine their specific or even unique chromatographic characteristics [42,43]. In conventional testing procedures for RP-HPLC columns these polar column properties are usually described with the general term “silanol activity”. In a recent overview of Nawrocki [44] and in another

comparative study on test methods for RP-HPLC columns by Claessens et al. [35], it has been shown that this term is rather poorly defined. From these studies it became obvious that “silanol activity” comprises a number of interactions of significantly different energy levels between analytes, stationary phases and eluents. Clearly distinguishing between the various polar contributions to the chromatographic column properties may significantly contribute to our understanding of the separation process and the classification of RP-HPLC columns. One of the specific aims of the present study is the detailed elucidation of the various contributions (e.g., the hydrogen-bond activities or dipolarity/polarizability) to the total “silanol activity” of a column via QSRR.

As regards polar retentivity of the columns under study, Table 8 shows that the net effect to retention provided by μ^2 is negative. This can be explained by assuming that the dipole–dipole and dipole–induced dipole attractions are stronger between the analyte and the polar molecules of eluent than between the same analyte and the non-polar hydrocarbon ligand of the stationary phase.

As illustrated in Fig. 5 there is quite a significant correlation ($R=0.7219$) between the coefficient k_3'' before μ^2 (Table 8) and the coefficient k_5' before β_2^H (Table 7). The coefficient k_5' is considered to reflect hydrogen-bond acidity of stationary phases. The total dipole moment tends to correlate with the ability of the analyte molecule to act as a hydrogen-bond acceptor, which may in general be reasonable.

Considering k_5' and k_3'' (Tables 7 and 8, Fig. 5) one can classify the phases NuC8, SelB, XC18, NuC18 as the most polar and the phases TPW, All, Alu, Puro, Sym8 as the least polar. With an exception for the Alu and TPW columns, this observation can be directly related to the differences in amount and activity of free silanols on individual stationary phases, which are accessible to analytes. The validity of this ranking is further supported (Tables 2 and 3) by the fact that the Alu (polybutadiene coated alumina) and TPW (methacrylate copolymer) columns are non-silica based packings. Also, the All column is a polymeric silica-based double endcapped phase, which impedes silanol accessibility at the surface. On the other hand, the SelB and NuC8

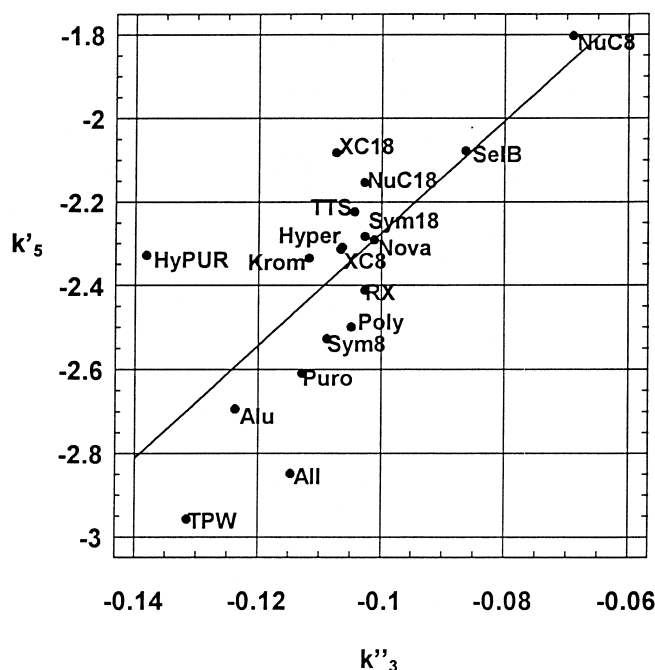


Fig. 5. Ordering of stationary phases according to their hydrogen-bond donor activity quantified by the coefficient k_5' for the β_2^H variable (Table 7) and total dipolarity quantified by the coefficient k_3'' for the μ^2 variable (Table 8) in QSRR equations employing the LSER-based and the molecular modeling-based structural descriptors of test analytes. Regression line k_5' vs. k_3'' is drawn between the column data points.

phases are non-encapped silica-based packings and hence most polar.

It proved interesting to compare the QSRR-based ranking of the columns according to their polarity with that provided by the conventional empirical testing methods [36–40]. Appropriate data were determined independently by Claessens et al. [35] for the same set of columns. The data set comprised of SAW – silanol activity defined as $k_{N,N\text{-diethyltoluamide}}/k_{\text{anthracene}}$ [36]; HBC – hydrogen-bonding capacity defined as $k_{\text{caffeine}}/k_{\text{phenol}}$ [37]; ASM – asymmetry of 4-ethylaniline at 5% of peak height [38,40]; SAG – silanol activity calculated from the ratio $k_{\text{aniline}}/k_{\text{phenol}}$ [39]. A correlation matrix for the QSRR-based and the conventional empirical column polarity parameters is given in Table 10.

It is clear from Table 10 that the proposed and the standard empirical column polarity parameter are not strongly intercorrelated. Hence, if reliable, they reflect different aspects of column polarity. Again, there is a lack of correlation among the conventional empirical testing methods despite their apparent similarity. Thus, none of them can be recommended. Interestingly, the column polarity parameter proposed here, k_3'' , correlates relatively well ($R=0.8325$) with the standard empirical parameter HBC defined by the ratio of retention factors of caffeine and phenol and called the hydrogen-bonding capacity parameter by the original authors [37]. Also, the QSRR-based parameter of hydrogen-bonding acidity

of columns, k_5' , shows a closer correlation with HBC than with other conventional empirical parameters.

We believe that the standard empirical column polarity parameters are combinations of several factors. They produce a column polarity ranking that changes with the change of test solutes. Contrastingly, the column dipolarity parameter, k_3'' , and the column hydrogen-bonding acidity parameter, k_5' , determined on a large series of analytes, are more “pure” column polarity parameters.

A more detailed analysis of column classification according to the ability to participate in specific types of polar interactions with analytes is less certain. The reason is that there are relatively large standard deviations of the remaining regression coefficients in QSRR equations, k_3'' and k_2'' (Tables 7 and 8; Figs. 6 and 7). However, the extreme positions of the columns according to their k_3' and/or k_2'' parameters seem to be reliable.

The positive sign for the δ_{min} term in QSRR equations in Table 8 appears to be logical; note that the δ_{min} values in Table 5 are negative (they reflect an electron excess in the most charged atom in an analyte molecule). The more charged an atom is, the higher the absolute value of the $k_2''\delta_{\text{min}}$ term is and thus the less retained the analyte is. At first we interpreted the δ_{min} parameter as reflecting the ability of analytes to form the electron-pair-donor/electron-pair-acceptor (EPD/EPA) complexes with other molecules. Such complexes would be more easily formed between the analytes and the molecules of eluent than with the chemically inert hydrocarbons of the stationary phases. In Fig. 6 the columns are ordered according to increasing polarity as reflected by k_2'' (Table 8). If this reflects their ability to form EPD/EPA complexes with analytes, then the highest potential for that is shown by the HyPUR column followed by the TPW, Sym18, Sym8 and NuC8 columns. The least polar with that respect are the All, Puro, Poly, Hyper and RX columns.

The coefficient k_3' at π_2^{H} could reflect the ability of the stationary phase to take part in dipole–dipole and dipole–induced dipole interactions with analytes (dipolarity/polarizability). There is no correlation between the coefficient k_3'' before μ^2 from Table 8 and the coefficient k_3' before π_2^{H} from Table 7. The ordering of columns according to k_3' , presented in Fig. 7, shows little agreement with the trend illustrated in Fig. 6.

Table 10

Correlation matrix for the parameters of polar retentivity of 18 stationary phases studied^a

R	k_5'	k_3''	SAW	HBC	ASM
k_3''	0.7219	1	0.6430	0.8325	0.3360
SAW	0.4118	0.6430	1	0.7160	0.1772
HBC	0.6591	0.8325	0.7160	1	0.3714
ASM	0.3785	0.3360	0.1772	0.7160	1
SAG	0.1708	0.4480	0.6317	0.6250	0.2886

^a Parameter k_5' is the regression coefficient for the hydrogen-bonding basicity of analyte, β_2^{H} (Table 7); k_3'' is the regression coefficient for the square of total dipole moment of analyte, μ^2 (Table 8); SAW is the parameter designed [36] to account for silanol activity of the stationary phase; HBC is the parameter designed [37] to account for the hydrogen-bonding capacity; ASM is the parameter designed [38,40] to account for silanol activity; SAG is another parameter designed [39] to account for the silanol activity of stationary phases. The numerical values of SAW, HBC, ASM and SAG for correlation analysis were taken from Claessens et al. [35].

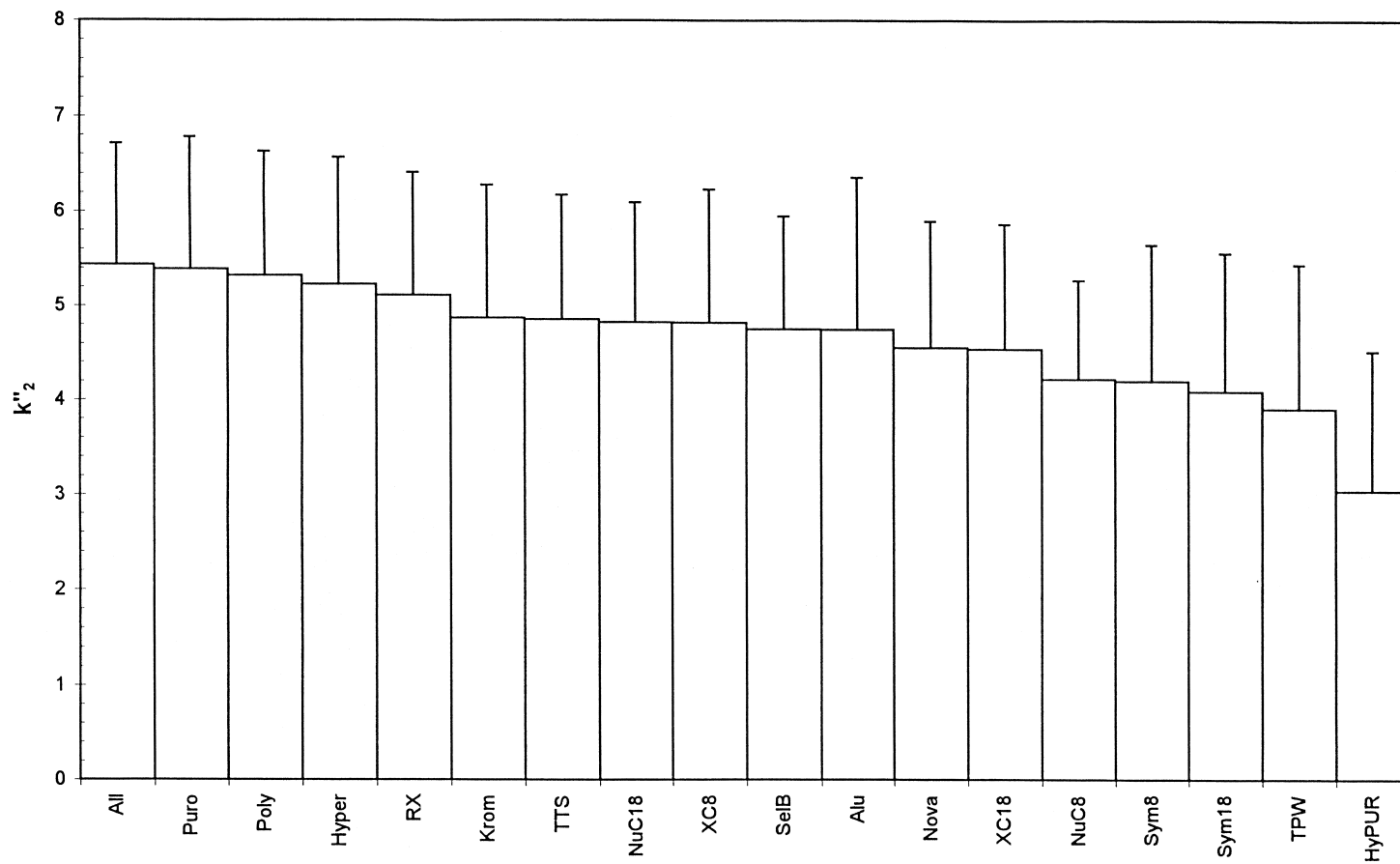


Fig. 6. Ordering of the columns studied according to their EPD/EPA polarity quantified by the coefficient k''_2 for the δ_{\min} variable (Table 8) in QSRR equations relating $\log k_w$ data from methanol–water systems to the structural descriptors from molecular modeling.

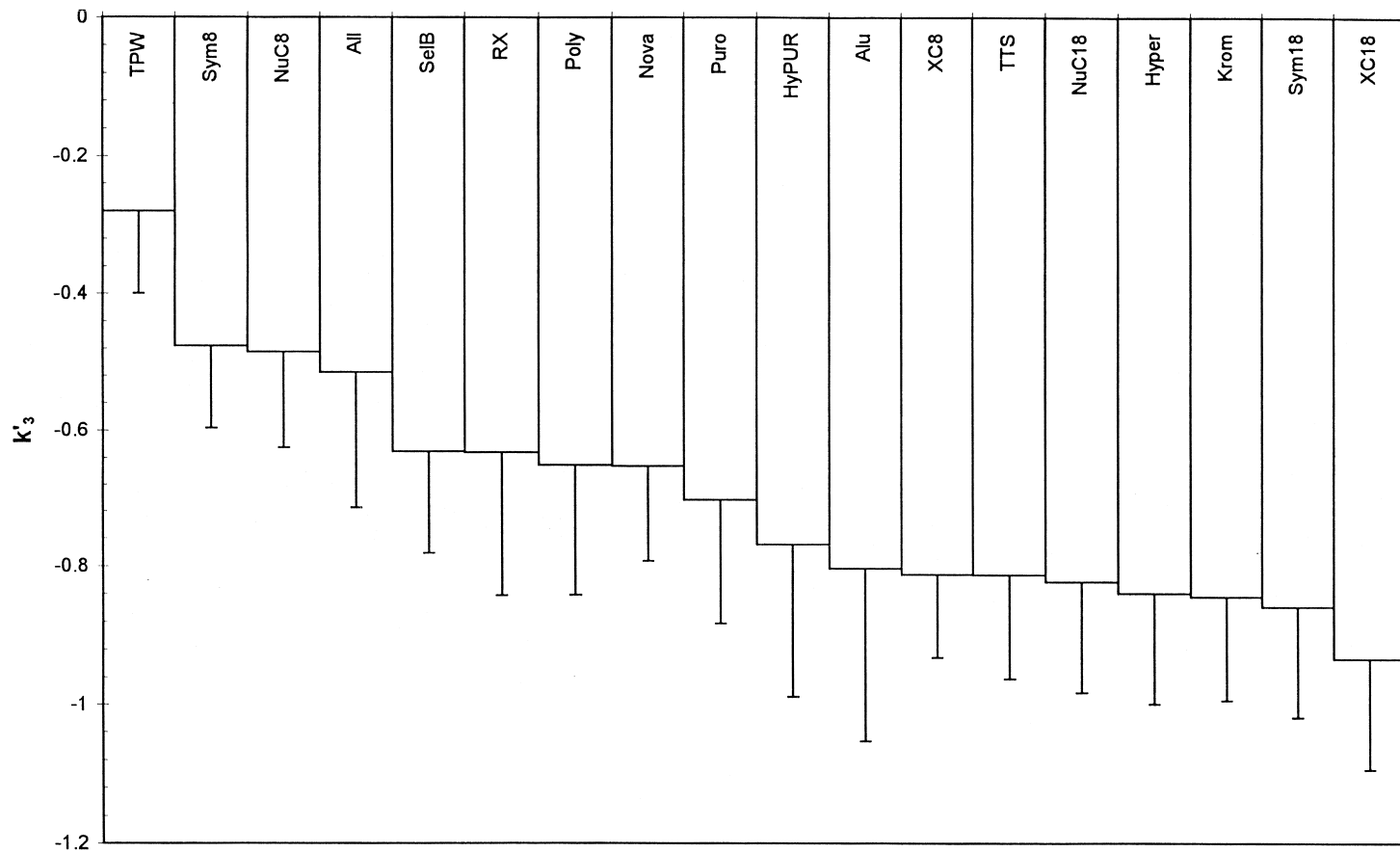


Fig. 7. Ordering of the columns studied according to their dipolarity/polarizability quantified by the coefficient k'_3 for the π_2^H variable (Table 7) in QSRR equations relating $\log k_w$ data from methanol–water systems to LSER-based structural descriptors.

If one attempted to classify the stationary phases studied according to their polarity accounted for by k'_3 , the most polar columns would be TPW, Sym8 and NuC8. The least polar appear to be XC18, Sym18, Krom and Hyper.

Physical meaning and reliability of the proposed individual parameters of stationary phases become even more convincing if one analyses such a complex property like hydrophobicity in terms of these parameters. Coming back to Table 6 and Fig. 3 one finds the NuC8 phase is the least lipophilic ($k_2 = 0.6268$, Table 6). This can be explained by the fact that it has the lowest non-specific London retentivity ($k'_6 = 2.8275$, Table 7; $k''_4 = 0.0152$, Table 8) on the one hand, and both the highest hydrogen-bond acidity and total dipolarity ($k'_5 = -1.8035$, Table 7; $k''_3 = -0.0690$, Table 8) and one of the highest dipolarity/polarizability and EPD/EPA polarity ($k'_3 = -0.4852$, Table 7; $k''_2 = 4.2158$, Table 8) on the other. The column SelB is a bit more hydrophobic than NuC8. Its k_2 equals 0.7274 (Table 6). SelB has higher London retentivity ($k'_6 = 3.1335$; $k''_4 = 0.0169$) than NuC8, lower hydrogen-bond acidity and total dipolarity ($k'_5 = -2.0788$; $k''_3 = -0.0863$) and lower dipolarity/polarizability and EPD/EPA polarity ($k'_3 = -0.6312$; $k''_2 = 4.7467$).

The Nova and Sym8 columns have equal and higher hydrophobicity than SelB ($k_2 = 0.7574$ and $k_2 = 0.7582$, respectively). The two C_8 columns have rather low non-specific dispersive London retentivity: the k'_6 for Nova is 3.0889 and 2.9831 for Sym8; respective k''_4 values are 0.0164 and 0.0154. These phases have reduced polarity, however. This is more evident in the case of Sym8 ($k'_5 = -2.5275$, $k''_3 = -0.1088$) and a bit less marked in the case of Nova ($k'_5 = -2.2913$, $k''_3 = -0.1012$). With respect to the non-hydrogen-bonding polarity and total dipolarity, Nova and especially Sym8 belong to more polar phases [k'_3 and k''_2 values are for Sym8 and Nova -0.4766 and -0.6525 (k'_3) and 4.1946 and 4.5518 (k''_2), respectively].

The properties of the methacrylate copolymer-based TPW phase are interesting. This phase shows the lowest non-specific retentivity of all the phases studied ($k'_6 = 2.8104$; $k''_4 = 0.0137$). It also has the lowest polarity as reflected by the hydrogen-bond donor capacity and total dipolarity ($k'_5 = -2.9580$; $k''_3 = -0.1315$). On the other hand, TPW has highest

dipolarity/polarizability and EPD/EPA polarity ($k'_3 = -0.280$; $k''_2 = 3.9018$). All together, TPW has medium hydrophobicity ($k_2 = 0.7874$).

The hydrophobicity of XC8, XC18, NuC18, TPW, TTS, HyPUR, RX, Sym18, Poly, Krom and Hyper is very similar. This can be explained in terms of the similarity and/or compensation of non-polar, polar hydrogen-bonding and polar non-hydrogen-bonding properties. Higher hydrophobic properties of All and Puro phases can be explained by relatively high non-specific retentivity of the phases (k'_6 equals 3.4395 and 3.3056, respectively; k''_4 equals 0.0186 and 0.0183, respectively) and one of the lowest hydrogen-bond acidity and total dipolarity (k'_5 equals -2.8494 and -2.6098 , respectively; k''_3 equals -0.1147 and -0.1129 , respectively). Besides that, the phases All and Puro exhibit the lowest EPD/EPA polarity marked with the largest k''_2 coefficients (k''_2 equals 5.4318 and 5.3904, respectively).

It must be noted here that the mechanism of retention for both All and Puro seems to differ from the majority of columns. As can be seen in Table 7, the QSRR describing $\log k_w$ from methanol–water eluents determined using the two stationary phases comprise an analyte hydrogen-bond acidity term (α_2^H), which is insignificant or of low significance for the remaining columns when methanol–water mobile phases are used. The α_2^H term is significant at $>95\%$ level (but less than 99%) for Poly and RX columns too. This could mean that the All and Puro phases possess marked, and Poly and RX possess minor hydrogen-bond acceptor properties (along with the hydrogen-bond donor properties observed for all phases).

A further comment is required regarding the hydrophobicity ($k_2 = 0.8741$) of the alumina-based column Alu; the largest of all the phases studied. This cannot be explained only from non-specific London retentivity represented by the relatively small values of k'_6 and k''_4 (2.9541 and 0.0162, respectively). In addition, it can also hardly be compensated by the low hydrogen-bonding polarity and total dipolarity of Alu, which are one of the lowest ($k'_5 = -2.6940$; $k''_3 = -0.1237$), and by dipolarity/polarizability and EPD/EPA polarity, which are medium ($k'_3 = -0.8036$; $k''_2 = 4.7425$). The QSRR equations for Alu given in Table 7 comprise a significant, positive excess molar refractivity term

(R_2), which is absent in the QSRR describing the silica-based phases. This term may indicate a molecular-size-related attraction of analytes by the alumina matrix of this stationary phase. This effect adds to the previously discussed interactions operating in the eluent–hydrocarbonaceous silica systems. A good correlation of $\log k_w$ determined on the alumina-based hydrocarbonaceous columns with $\log P$ has already been noted [45].

4. Conclusions

QSRR analysis of organic modifier logarithms of retention factor standardized to zero percent, i.e. $\log k_w$, for a designed series of structurally diverse test analytes allows for a rationalization of the molecular mechanism of separation operating in given RP-HPLC systems. In view of statistically significant and physically meaningful QSRR equations, it was possible to explain the often observed differences in retention in objective, numerical terms, due to the nature of both the mobile and the stationary phase. Three types of QSRR employing the empirical and the calculation chemistry structural descriptors allowed for the rationalization of the molecular mechanism of retention and classification of modern hydrocarbon-silica RP-HPLC materials according to the type and magnitude of intermolecular interactions affecting the retention.

The present study confirms the ability of QSRR analysis to identify stationary phases, which show distinctively different retention mechanisms from that typically observed for RP-HPLC columns. This has been proven by the statistical significance of specific structural descriptors in QSRR equations concerning these atypical columns. Hence, the Alu column was distinguished from the remaining ones due to the significance of the excess molar refractivity descriptor (R_2) in LSER-based QSRR equations. The significance of the α_2^H term in QSRR equations distinguishes a subgroup of four C_{18} columns (All, Puro, RX and Poly).

Comparing the stationary phases in terms of the ability to reflect hydrophobicity of analytes (as expressed by $\log P$) gives limited information about fundamental interactions determining separations on individual phases. As regards the correlation of

retention of test analytes on individual phases to $\log P$, the differences among most phases are insignificant. Some exceptions are Alu, All and Puro that best mimic the octanol–water partition; NuC8 and SelB are the worst ones in that respect.

The magnitude of regression coefficients for individual structural descriptors in QSRR equations allows us to order stationary phases. A definite physical sense can be assigned to the coefficient for the molecular-bulkiness descriptors of test analytes. These coefficients quantify the ability of stationary phases to participate in London-type dispersion interactions and characterize non-polar (London) retentivity of the column. This was confirmed by two types of QSRR equations; the columns studied were ordered accordingly. The most retentive columns were All, XC18, RX and Hyper. The least retentive non-specifically appeared to be TPW, NuC8, Alu and Sym8.

With the magnitude of coefficients for the descriptors of analyte polarity in QSRR equations in mind, the phases were ordered according to their hydrogen-bond donor and total dipolarity properties. These properties are probably connected with accessibility to analyte of free silanols of the stationary phase.

The measures of EPD/EPA polarity and dipolarity/polarizability of stationary phases can also be suggested based on QSRRs, but these effects seem to be of minor importance for retention regarding most of the hydrocarbonaceous phases studied. Their significance for stationary phase characterization could be more convincingly proved if phases comprising diverse functionalities were compared.

Interpretation of the observed organic–water partition properties of the columns under study (as expressed by their hydrophobicity parameter, k_2) is feasible in terms of the proposed measures of their non-polar and polar retentivity. Hence, the approach proposed here can be of help in the rational development of new stationary phase materials of requested partition characteristics.

It must be noted here that the statistical quality of some QSRR equations does not allow us to differentiate decisively between all the columns. Some columns are very similar and the lack of significant differences in QSRR is confirmed by the similar retention patterns given by these columns. Some

QSRRs that indicate the actual differences are of relatively low significance. Their value has been confirmed here by another type of QSRR showing similar regularity.

In general, the QSRR approach for testing the columns for RP-HPLC provided reliable, objective, quantitative, and physically interpretable results as opposed to the conventional empirical testing methods.

Acknowledgements

The authors gratefully acknowledge Dr. M. Sieber (Macherey-Nagel), Dr. J.J. Kirkland (Hewlett-Packard), Dr. U.D. Neue (Waters), Dr. D. Sanchez (EKA Nobel), Mr. M. Krause (TosoHaas) and Mr. M. Verstegen (Alltech), Dr. P. Ross (Shandon) and Dr. G. Wieland (Merck) for making the columns and product information available for use in this study. This work was partially carried out under Grant 4P05F 004 15 (R.K., M.M.) from the Komitet Badań Naukowych, Warsaw, Poland.

References

- [1] R. Kaliszán, *Structure and Retention in Chromatography. A Chemometric Approach*, Harwood Academic Publishers, Amsterdam, 1997.
- [2] R. Kaliszán, *Anal. Chem.* 64 (1992) 619A.
- [3] B.J. Herbert, J.G. Dorsey, *Anal. Chem.* 67 (1995) 744.
- [4] A. Pagliara, E. Khamis, A. Trinh, P.A. Carrupt, R.-S. Tsai, B. Testa, *J. Liq. Chromatogr.* 18 (1995) 1721.
- [5] M.H. Abraham, H.S. Chadha, R.A.E. Leitao, R.C. Mitchell, W.J. Lambert, R. Kaliszán, A. Nasal, P. Haber, *J. Chromatogr. A* 766 (1997) 35.
- [6] P.C. Sadek, P.W. Carr, R.M. Doherty, M.J. Kamlet, R.W. Taft, M.H. Abraham, *Anal. Chem.* 57 (1985) 2971.
- [7] P.W. Carr, *Microchem. J.* 48 (1993) 4.
- [8] P.W. Carr, R.M. Doherty, M.J. Kamlet, R.W. Taft, W. Melander, C. Horvath, *Anal. Chem.* 58 (1986) 2674.
- [9] L.C. Tan, P.W. Carr, M.H. Abraham, *J. Chromatogr. A* 752 (1996) 1.
- [10] A. Nasal, P. Haber, R. Kaliszán, E. Forgács, T. Cserhádi, M.H. Abraham, *Chromatographia* 43 (1966) 484.
- [11] M.H. Abraham, M. Ross, C.F. Poole, S.K. Poole, *J. Phys. Org. Chem.* 10 (1997) 358.
- [12] K. Valko, N. Plass, C. Bevan, D. Reynolds, M.H. Abraham, *J. Chromatogr. A* 797 (1998) 41.
- [13] A. Sandi, L. Szepeszy, *J. Chromatogr. A* 818 (1998) 1.
- [14] A. Sandi, L. Szepeszy, *J. Chromatogr. A* 818 (1998) 19.
- [15] B.C. Cupid, J.K. Nicholson, P. Davis, R.J. Ruane, I.D. Wilson, R.C. Glen, V.S. Rose, C.R. Beddell, J.C. Lindon, *Chromatographia* 37 (1993) 241.
- [16] K. Azzaoui, L. Morin-Allory, *Chromatographia* 42 (1996) 389.
- [17] B. Buszewski, R. Gadzala-Kopciuch, M. Markuszewski, R. Kaliszán, *Anal. Chem.* 69 (1997) 3277.
- [18] M.H. Abraham, *Chem. Soc. Rev.* 22 (1993) 73.
- [19] M.H. Abraham, University College London Data Base, 1996.
- [20] P.N. Craig, in: C. Hansch, P.G. Sammes, J.B. Taylor (Eds.), *Comprehensive Medicinal Chemistry*, Vol. 6, Pergamon Press, Oxford, 1990.
- [21] C. Hansch, A. Leo, D. Hoekman, *Exploring QSAR. Hydrophobic, Electronic, and Steric Constants*, ACS, Washington, DC, 1995.
- [22] M. Charton, S. Clementi, S. Ehrenson, O. Exner, J. Shorter, S. Wold, *Quant. Struct.-Act. Relat.* 4 (1985) 29.
- [23] E. Soczewinski, C.A. Wachtmeister, *J. Chromatogr.* 7 (1962) 311.
- [24] T.H. Dzido, H. Engelhardt, *Chromatographia* 39 (1994) 51.
- [25] R.M. McCormick, B.L. Karger, *Anal. Chem.* 52 (1980) 2249.
- [26] R.S. Helburn, S.C. Rutan, J. Pompano, D. Mitchem, W.T. Patterson, *Anal. Chem.* 66 (1994) 610.
- [27] Cs. Horváth, W. Melander, J. Molnar, *J. Chromatogr.* 125 (1976) 129.
- [28] J.H. Knox, R. Kaliszán, G.J. Kennedy, *J. Chem. Soc., Faraday Symp.* 15 (1980) 113.
- [29] H. Engelhardt, M. Arangio, T. Lobert, *LC·GC Int.* 10 (1997) 803, and references therein.
- [30] K. Miyake, N. Mizuna, H. Terada, *J. Chromatogr.* 439 (1988) 227.
- [31] P.M. Sherblom, R.P. Eganhouse, *J. Chromatogr.* 454 (1988) 37.
- [32] T. Braumann, B. Jastorff, *J. Chromatogr.* 350 (1985) 105.
- [33] K.A. Dill, *J. Phys. Chem.* 91 (1987) 1980.
- [34] J.H. Knox, P. Ross, *Adv. Chromatogr.* 37 (1997) 73.
- [35] H.A. Claessens, M.A. Straten, C.A. van Cramers, M. Jezierska, B. Buszewski, *J. Chromatogr. A* 826 (1998) 135.
- [36] M.J. Walters, *J. Assoc. Off. Anal. Chem.* 70 (1987) 465.
- [37] K. Kimata, K. Iwaguchi, S. Onishi, K. Jinno, R. Eksteen, K. Hosoya, M. Araki, N. Tanaka, *J. Chromatogr. Sci.* 27 (1989) 721.
- [38] H. Engelhardt, M. Jungheim, *Chromatographia* 29 (1990) 59.
- [39] S.V. Galushko, *Chromatographia* 36 (1993) 39.
- [40] H. Engelhardt, M. Arangio, T. Lobert, *LC·GC Int.* 15 (1997) 856.
- [41] S.V. Galushko, A.A. Kamenchuk, G.L. Pit, *J. Chromatogr. A* 660 (1994) 47.
- [42] L. Nondek, B. Buszewski, D. Berek, *J. Chromatogr.* 360 (1986) 241.
- [43] P. Chan Leach, M.A. Stadalius, J.S. Berus, L.R. Snyder, *LC·GC Int.* 1 (1988) 22.
- [44] J. Nawrocki, *J. Chromatogr. A* 779 (1997) 29.
- [45] R. Kaliszán, R.W. Blain, R.A. Hartwick, *Chromatographia* 25 (1988) 5.